Cancellation of Grating Lobes in Scanned Linear Antenna Arrays using Genetic Algorithm

by

Syed Tariq Magrabi

A Thesis Presented to the

FACULTY OF THE COLLEGE OF GRADUATE STUDIES

KING FAHD UNIVERSITY OF PETROLEUM & MINERALS

DHAHRAN, SAUDI ARABIA

In Partial Fulfillment of the
Requirements for the Degree of

MASTER OF SCIENCE

In

ELECTRICAL ENGINEERING

May, 1998

INFORMATION TO USERS

This manuscript has been reproduced from the microfilm master. UMI films the text directly from the original or copy submitted. Thus, some thesis and dissertation copies are in typewriter face, while others may be from any type of computer printer.

The quality of this reproduction is dependent upon the quality of the copy submitted. Broken or indistinct print, colored or poor quality illustrations and photographs, print bleedthrough, substandard margins, and improper alignment can adversely affect reproduction.

In the unlikely event that the author did not send UMI a complete manuscript and there are missing pages, these will be noted. Also, if unauthorized copyright material had to be removed, a note will indicate the deletion.

Oversize materials (e.g., maps, drawings, charts) are reproduced by sectioning the original, beginning at the upper left-hand corner and continuing from left to right in equal sections with small overlaps. Each original is also photographed in one exposure and is included in reduced form at the back of the book.

Photographs included in the original manuscript have been reproduced xerographically in this copy. Higher quality 6" x 9" black and white photographic prints are available for any photographs or illustrations appearing in this copy for an additional charge. Contact UMI directly to order.

UMI

A Bell & Howell Information Company
300 North Zeeb Road, Ann Arbor MI 48106-1346 USA
313/761-4700 800/521-0600

CANCELLATION OF GRATING LOBES IN SCANNED LINEAR ANTENNA ARRAYS USING GENETIC ALGORITHM

BY

SYED TARIQ MAGRABI

A Thesis Presented to the

FACULTY OF THE COLLEGE OF GRADUATE STUDIES

KING FAHD UNIVERSITY OF PETROLEUM & MINERALS

DHAHRAN, SAUDI ARABIA

In Partial Fulfillment of the
Requirements for the Degree of

MASTER OF SCIENCE
In
ELECTRICAL ENGINEERING

MAY 1998

UMI
300 North Zeeb Road
Ann Arbor, MI 48103

KING FAHD UNIVERSITY OF PETROLEUM AND MINERALS

DHAHRAN, SAUDI ARABIA

COLLEGE OF GRADUATE STUDIES

This thesis, written by

SYED TARIQ MAGRABI

under the direction of his Thesis Advisor and approved by his Thesis Committee, has been presented to and accepted by the Dean of the College of Graduate Studies, in partial fulfillment of the requirements for the degree of

MASTER OF SCIENCE IN ELECTRICAL ENGINEERING

Thesis Committee

Mahmoud M. Dawoud 8/6/1998

Dr. Mahmoud M. Dawoud (Chairman)

June 8 1998

Dr. Samir Abdul Jauwad (Member)

H. A. Ragheb

Dr. Ragheb Hassan Aly (Member)

A. Hamid

Dr. Abdul Kadir Hamid (Member)

8/6/98

Dr. Samir Al – Baiyat
(Department Chairman)

Dr. Abdallah M. Al – Shehri
(Dean, College of Graduate Studies)

22/6/98
Date

Dedicated to

my most loving Mamma

Acknowledgements

This work is an expression of my gratitude to Allah (swt). May Allah bestow peace on his Prophet, Muhammad (pbuh).

The following few lines are for my Advisor Dr. Mahmoud M Dawoud. Put in simple words, he has been an ideal teacher. It was because of him that the work at any point of time, never got stressful. Each time I went to meet him for the most trivial of problems, he gave me a patient hearing and tried his best to come down to my level to explain things. Thanks a lot Sir.

My learned commitee of Dr Samir Abdul Jauwad, Dr. Hassan Ali Ragheb and Dr Hamid were a pleasure to work with. They gave suggestions that made this work even better.

My family, especially my most loving Mamma, Pappa and Baji were a constant source of motivation. Their love carried me through some difficult moments. A profound acknowledgement of the effort of my grandparents and LQ uncle is too short for words.

KFUPM has provided me with some of the most cherished moments thanks

entirely due to the Resarch Assistant community. They made my stay over here memorable, and joyous. I had the fortune of living in the most boisterous house in NC and hopefully with that experience I can be on my own anywhere.

Although some people didnt contribute directly to this effort, I still would like to acknowledge their role. My best friend Zakir, despite his tough schedule at INTEL, did his best to bring me to the lab with his e-mails. The speed of completion is entirely due to his wake up calls. I would also like to thank Ahsan, Mohsin, Pasha, Moiz and Hussain who have helped me in crucial times during this research.

Contents

Acknowledgements i

List of Tables viii

List of Figures xv

Abstract (English) xvi

Abstract (Arabic) xvii

1 INTRODUCTION 1

1.1 Null Steering 3

1.2 Overview of Genetic Algorithms 4

1.2.1 Genetic Operators 6

1.2.2 Parent Selection 7

1.2.3 Fitness Function 8

1.3 Literature Review 8

1.3.1 Analytical Null Steering Methods 9

1.3.2 Null steering based on the Genetic Algorithm 11

1.3.3 Grating lobes and their suppression 13

1.4 Objectives of the Work 14

2 An Overview of linear arrays **17**

2.1 Linear Arrays 17

2.1.1 Phased Arrays 19

2.2 Effects of Changing Array Parameters 20

2.2.1 Grating Lobes 22

2.2.2 Effect of Grating Lobes on Directivity 23

2.3 Appearance of grating lobes for a 10 element array 23

2.4 Brief description of analytical null steering methods 25

2.4.1 Element position perturbations 25

2.4.2 Complex weights 26

2.5 Directivity calculation 27

3 The genetic algorithm as applied to grating lobe control **29**

3.1 Introduction 29

3.2 Program Description 29

3.3 Description of Routines 31

3.3.1 Initialization 33

3.3.2 Generating Initial Population 34

3.3.3 Fitness Function 34

3.3.4 Parent Selection 37

3.3.5 Crossover Operation 37

3.3.6 Mutation Operation 38

3.3.7 Sorting of Chromosomes 40

4 Results and Discussion **42**

4.1 Use of position perturbations 43

4.1.1 Effects of increasing inter-element spacing with main beam at 70^0 46

4.1.2 Main beam at 20^0 50

4.2 Application to 20 and 32 element arrays 52

4.3 Complex Weight perturbations 56

4.3.1 Main beam at 60^0 59

4.3.2 Main beam at 70^0 62

4.3.3 Application to a 20 element array 65

4.4 Application to Chebyshev arrays 65

4.5 Effect of grating lobe control on Directivity 74

4.5.1 Directivity analysis for Chebyshev arrays 78

5 Effect of element pattern on grating lobe control **80**

5.1 Introduction 80

5.2 Finite length dipole 81

5.2.1 Current distribution 81

5.2.2 Radiated fields: Element factor, Space factor and Pattern multiplication 81

5.3 Effect of increasing the length of dipole 85

5.3.1 Scanning the element pattern 88

5.4 Application of Element pattern and Array factor pattern for grating lobe control 91

5.4.1 Application to a 12 element 0.75λ spaced array 91

5.4.2 Application to 12 element, 0.8λ spaced array 94

5.4.3 Application to a 20 element array 96

5.4.4 Application to a Chebyshev array 97

5.5 Discussion 98

6 Conclusions and Recommendations **101**

6.1 Conclusion 101

6.2 Recommendations 105

Bibliography **105**

Vita **111**

List of Tables

3.1 String representation 30

4.1 Perturbations corresponding to Figure 4.1 in terms of λ 45

4.2 Perturbations corresponding to Figure 4.2 in terms of λ 47

4.3 Perturbations corresponding to Figure 4.3 in terms of λ 49

4.4 Perturbations corresponding to Figure 4.4 in terms of λ 51

4.5 Perturbations corresponding to Figure 4.5 in terms of λ 51

4.6 Perturbations corresponding to Figure 4.6 in terms of λ 54

4.7 Perturbations corresponding to Figure 4.7 in terms of λ 55

4.8 Perturbations corresponding to Figure 4.9 57

4.9 Perturbations corresponding to Figure 4.10 58

4.10 Perturbations corresponding to Figure 4.11 60

4.11 Perturbations corresponding to Figure 4.12 61

4.12 Perturbations corresponding to Figure 4.13 63

4.13 Perturbations corresponding to Figure 4.14 63

4.14 Perturbations corresponding to Figure 4.15 64

4.15 Perturbations corresponding to Figure 4.16 66

4.16 Perturbations corresponding to Chebyshev Figure 4.17 69

4.17 Perturbations corresponding to Chebyshev Figure 4.18 in terms of λ . 71

4.18 Perturbations corresponding to Chebyshev Figure 4.19 in terms of λ . 72

4.19 Perturbations corresponding to Chebyshev Figure 4.20 73

4.20 Directivity for a 12 element array with main beam at 70^0 (using Complex Weights) 75

4.21 Directivity for a 12 element array with main beam at 70^0 (using Position perturbations) 76

4.22 Directivity for a 20 element Chebyshev array with main beam at 80^0 (using Position perturbations) 78

5.1 Table showing the variation of null positions for different dipole lengths when $\alpha = 20^0$. 93

List of Figures

1.1 Block diagram of a simple Genetic algorithm 5

2.1 Far field geometry of N element array of isotropic sources positioned along the z-axis. 18

2.2 Pattern showing the appearance of a Grating lobe at 132^0 for a 10 element array with inter element separation d=0.85λ. 22

2.3 Plot showing the position of grating lobes for a 10 element array when main beam is directed to 20^0, 30^0, 50^0, and 85^0 24

2.4 Plot showing the variation of directivity for a 10 element array. 28

3.1 Flow chart of the Genetic algorithm as applied to the problem 32

3.2 Flow chart of the Initialization routine 33

3.3 Flow chart showing the evaluation of Fitness Function 36

3.4 Flow chart showing the methodology for selecting parents 38

3.5 Flow chart showing the Crossover operation 39

3.6 Flow chart showing the Mutation operation 40

3.7 Flow chart showing the Sort operation 41

4.1 Array Factor Pattern for N=12, and separation=0.5λ with nulls imposed at 140^0 and 160^0. Dotted lines show the Original Pattern. . . . 45

4.2 Array Factor Pattern for N=12, and separation=0.5λ with nulls imposed at 140^0 and 160^0 with main beam at 70^0. Dotted lines show the Original Pattern. 47

4.3 Array Factor Pattern for N=12, and separation=0.6λ with nulls imposed at 120^0 and 170^0. Control level specified is $-60dB$. 48

4.4 Array Factor Pattern for N=12, and separation=0.75λ with nulls imposed at 160^0 and 170^0. Control level specified is $-15dB$. 49

4.5 Array Factor Pattern for N=12, and separation=0.8λ with nulls imposed at 150^0 and 160^0. Control level specified is $-15dB$. 50

4.6 Array Factor Pattern for N=12, and separation=0.5λ with nulls imposed at 145^0 and 170^0 with main beam at 20^0. Dotted lines show the Original Pattern. 52

4.7 Array Factor Pattern for N=20, and separation=0.75λ with nulls imposed at 144^0 and 148^0 with main beam at 60^O. Dotted lines show the Original Pattern. 53

4.8 Array Factor Pattern for N=32, and separation=0.75λ with nulls imposed at 145^0 and 147^0 with main beam at 60^O. Dotted lines show the Original Pattern. 54

4.9 Array Factor Pattern for N=12, and separation=0.5λ with nulls imposed at 140^0 and 160^0. Dotted lines show the Original Pattern. . . 57

4.10 Array Factor Pattern for N=12, and separation=0.5λ with nulls imposed at 115^0, 140^0 and 160^0 with main beam at 50^0. Dotted lines show the Original Pattern. 58

4.11 Array Factor Pattern for N=12, and separation=0.5λ with grating lobe control at 170^0 and 180^0 for the end-fire array. Dotted lines show the original pattern. 59

4.12 Array Factor Pattern for N=12, and separation=0.55λ with nulls of depth $-60dB$ imposed at 120^0 and 160^0 . Dotted lines show the Original Pattern. 60

4.13 Array Factor Pattern for N=12, and separation=0.68λ with lobe control imposed at 155^0, 170^0 and 180^0 with main beam at 60^0. Dotted lines show the Original Pattern. 61

4.14 Array Factor Pattern for N=12, and separation=0.6λ with lobe control imposed at 145^0 and 160^0 with main beam at 70^0. Dotted lines show the original pattern. 62

4.15 Array Factor Pattern for N=12, and separation=0.75λ with nulls imposed at 160^0 and 170^0 with main beam at 70^0. Dotted lines show the Original Pattern. 64

4.16 Array Factor Pattern for N=20, and separation=0.85λ with lobes controlled at 140^0, 160^0 and 172^0 with main beam at 80^0. Control level chosen is $-15dB$. Dotted lines show the Original Pattern. . . . 65

4.17 Array Factor Pattern for N=20, and separation=0.5λ with nulls imposed using complex weight perturbations at 145^0 and 160^0 with main beam at 90^0 and Control level chosen is $-60dB$. 68

4.18 Array Factor Pattern for N=20, and separation=0.5λ with nulls imposed using position perturbations at 145^0 and 160^0 with main beam at 90^0 and Null depth chosen is $-60dB$. 70

4.19 Array Factor Pattern for N=20, and separation=0.85λ with nulls imposed using position perturbations at 165^0 and 175^0 with main beam at 80^0 and Control level chosen is $-15dB$. 70

4.20 Array Factor Pattern for N=20, and separation=0.85λ with nulls imposed using complex weight perturbations at 165^0 and 175^0 with main beam at 80^0 and Control level chosen is $-15dB$. 74

4.21 Directivity plot for a 12 element array whose main beam is at 70^0. Complex weights are used for null steering 76

4.22 Directivity plot for a 12 element array whose main beam is at 70^0 and position perturbations are used for null steering 77

4.23 Directivity plot for a 20 element Chebyshev array whose main beam is at 80^0 and position perturbations are used for lobe control 79

5.1 An array of dipoles placed at an angle α with respect to z-axis . . . 84

5.2 Element patterns of a dipole as its length is varied from1.0λ to 1.05λ. For Fig (a)L=1.0λ. For Fig (b) L=1.01λ. For Fig (c) L=1.02λ, For Fig (d) L=1.03λ. For Fig (e) L=1.04λ. and For Fig (f) L=1.05λ . . . 86

5.3 Element patterns of a dipole as its length is varied from1.06λ to 1.1λ. for Fig (g) L=1.06λ. for Fig (h) L=1.07λ. for Fig (i) L=1.08λ. for Fig (j) L=1.09λ. and for Fig (k) L=1.1λ 87

5.4 Element pattern of a dipole of length 1.25λ. 87

5.5 Element patterns of a dipole of length 1.04λ. Fig (a) is for $\alpha = 0^0$ Fig (b) is for$\alpha = 20^0$. Fig (c) is for $\alpha = 40^0$, Fig (d) is for $\alpha = 70^0$ and Fig (e) is for $\alpha = 90^0$. 89

5.6 Element patterns of a dipole of length 1.05λ. Fig (a) is for $\alpha = 0^0$ Fig (b) is for$\alpha = 20^0$, Fig (c) is for $\alpha = 40^0$, Fig (d) is for $\alpha = 70^0$ and Fig (e) is for $\alpha = 90^0$. 90

5.7 Element pattern of a dipole of length 1.09λ with $\alpha = 20^0$. 90

5.8 Radiation pattern of a 12 element array of dipoles, each of length 1.03λ and having array factor nulls at 160^0 and 170^0. Inter element spacing is 0.75λ. Dotted lines show the unperturbed array factor pattern 92

5.9 Radiation pattern of a 12 element array of dipoles, each of length 1.03λ. Inter element spacing is 0.75λ. Dotted lines show the array factor pattern. 93

5.10 Radiation pattern of a 12 element array of dipoles, each of length 1.05λ and having array factor nulls at 150^0 and 160^0. Inter element spacing is 0.8λ. Dotted lines show the unperturbed array factor pattern 95

5.11 Radiation pattern of a 12 element array of dipoles, each of length 1.05λ. Inter element spacing is 0.8λ. Dotted lines show the array factor pattern. 96

5.12 Radiation pattern of a 20 element array of dipoles, each of length 1.04λ and having array factor nulls at 144^0 and 148^0. Inter element spacing is 0.75λ. Dotted lines show the original array factor pattern. 97

5.13 Radiation pattern of a 20 element array of dipoles, each of length 1.04λ. Inter element spacing is 0.75λ. Dotted lines show the array factor pattern. 98

5.14 Radiation pattern of a 20 element Chebyshev array of dipoles, each of length 1.005λ and having array factor nulls at 165^0 and 175^0. Inter element spacing is 0.85λ. Dotted lines show the original array factor pattern. 99

Abstract

Name: Syed Tariq Magrabi

Title: Cancellation of grating lobes in Scanned Linear Antenna Arrays using Genetic Algorithm.

Major Field: Electrical Engineering

Date of Degree: May, 1998

Genetic algorithms have been applied for null steering to control grating lobes in scanned arrays. Element position perturbations and complex-weight variations are the two techniques used for null steering. The use of genetic algorithm for null steering provides grating lobe control at the specified directions. Further control of the grating lobe has been achieved by the appropriate choice of the element pattern of finite length dipoles. Results presented for both uniform and non-uniform arrays, using the GA based control as well as control based on element pattern synthesis show that when these techniques are combined, good radiation patterns are obtained. This research has also shown that by controlling grating lobes, the directivity and the useful scanning range of the array increases. Null steering to control grating lobes does not affect the main beam. It is thus concluded from this research that the genetic algorithm can be an effective tool for designing scanned arrays with controlled grating lobes.

Master of Science Degree

King Fahd University of Petroleum and Minerals

Dhahran, Saudi Arabia

May, 1998

ملخص الرسالة

اسم الطالب: سيد طارق مغربي .

عنوان الرسالة: الغاء الفصوص الجانبية في المصفوفات الهوائية الخطية ذات المسح باستعمال الخوارزميات الوراثية.

لقد طبقت الخوارزميات الوراثية (Genetic Algorithms) لتوجيه انعدامية الأشعاع في التحكم في الفصوص الجانبية ذات التأثير السلبي في المصفوفات ذات المسح .يعتبر اضطراب مكان أعضاء المصفوفات الهوائية والتغير المركب للعوامل .الطريقتان شائعتا الأستعمال لتوجيه انعدامية الأشعاع.ان استعمال الخوارزميات الوراثية لتوجيه انعدام الاشعاع يمكن من التحكم في الفصوص الجانبية في الاتجاهات المحددة سابقا.لقد مكنت الطريقة المقترحة ففي التحكم أكثر في الفصوص الجانبية عن طريق الاختيار الأمثل لنمط اشعاع أعضاء المصفوفة ذات هوائي ثنائي القطب بطول محدد. أثبتت نتائج الدراسة في حالتي المصفوفات الهوائية المتسقة وغير المتسقة باستعمال الخوارزميات الوراثية في التحكم وطريقة التحكم بتحليل نمط اشعاع أعضاء المصفوفات,أنه بدمج الطريقتين يمكن الحصول علي نتائج أفضل. كما أثبتت هذه الدراسة أنه يمكن توسيع رقعة توجيه المصفوفات الهوائية والمسافة الفعلية للمسح. ان توجيه انعدامية الاشعاع للتحكم في الفصوص الجانبية لايؤثر علي الفص الرئيسي للمصفوفة ذات مسح وفصوص جانبية قليلة التأثير.

درجة الماجستير في العلوم

جامعة الملك فهد للبترول والمعادن

الظهران–المملكة العربية السعودية

محرم ١٤١٩ هـ

Chapter 1

INTRODUCTION

An antenna is a device for radiating or receiving radio waves. In other words, an antenna is the transitional structure between free space and a guiding device. In addition to receiving or transmitting energy, an antenna is usually required to optimize or accentuate radiation energy in some directions and suppress it in others. Thus an antenna must act as a directional device in addition to being a probing device.

Many applications require radiation characteristics that may not be achievable by a single antenna element. It may, however, be possible that with an aggregate or an array of radiating elements in an electrical and geometrical arrangement, radiation from the elements adds up to give a radiation maximum in a particular direction or directions, minimum in others. Antenna arrays provide this feature of pattern control. Due to this reason, extensive research has been done on their synthesis and

characteristics [1].

Antenna arrays are often required for many radar and communication applications. Some of these applications are direction finding and navigation. One feature of antenna arrays that makes them useful is their possession of beam steering capabilities, which is important in scanned and phased arrays.

The radiation pattern of an antenna element, defined as a graphical representation of the radiation properties as a function of space coordinates, is relatively wide, and hence, provides a low value of directivity. In many applications such as long distance communications it is necessary to design antennas that are very directive. Enlarging the dimensions of the antenna without physically increasing the size of the individual elements is done by forming an assembly of radiating elements in an electrical and geometrical configuration, known as an array. In an array of identical elements, there are five controls that can be used to shape the overall pattern of the antenna. These are :

- Array geometrical configuration (linear, circular, etc)
- The relative displacement between the elements
- The excitation phase of the individual elements
- The excitation amplitude of the individual elements
- The relative pattern of the individual elements

1.1 Null Steering

The chief objective of steering nulls in the antenna array pattern in the direction of interference sources is to cancel such sources. This cancellation is necessary in today's environment because of the immense importance given to satellite and mobile communications.

Null steering in antenna arrays can be achieved by controlling the complex weights, i.e. element amplitude and phase, amplitudes only, phase only or element positions. Several analytic solutions have been developed and utilized in order to determine the required changes in such parameters, so as to steer nulls in the required interference directions and to achieve acceptable level of null depth [2].

The first method, called complex weight control is very effective [3], and achieves null steering by changing both the phase and amplitude of the current in each antenna array element. The number of degrees of freedom in this case is twice the number of array elements, resulting in better control of null steering. On the other hand, it increases the array design complexity and can be comparatively slow due to the large number of variables that have to be determined [3]. Array pattern nulling can be achieved by phase only or element position variations, in which cases, the number of steered nulls must be less than half the total number of array elements. Many analytic solutions and methods such as Least Squares and Downhill Simplex can be used to steer nulls, but the genetic algorithm may be more suitable, because

as suggested in literature, it is more likely to converge to a global minima [3].

1.2 Overview of Genetic Algorithms

Genetic Algorithms are robust search techniques that mimic the basic principles of natural selection and biological evolution. The Genetic Algorithm was first articulated by Holland in 1973 [4]. Since then, a lot of attention has been given to this approach because of its great potential to address combinatorial optimization problems.

Domain knowledge is embedded in the abstract representation of a candidate solution termed as a *chromosome*. Each chromosome is made up of units called *genes*, representing the individual variables. Chromosomes are grouped, judiciously, into sets called *population*. The population at a given stage is referred to as *generation*. The survival of a chromosome is judged by its *fitness value*. The fitness value of each chromosome is obtained by a *fitness function* which evaluates the chromosome with respect to the objective function of the on-hand optimization problem. The fitter chromosomes have a higher probability of getting *selected*. These selected chromosomes are called *parents* which represent feasible solutions. Parents are mated (usually, in pairs) to produce new strings of feasible solutions called *offspring/children*. The block diagram of a simple genetic algorithm is given in figure 1.1. There are three main steps in this algorithm which have been the subject of

many research works right from its inception. These important operations are:

- Creating new chromosomes by mating current chromosomes via the reproduction operators.
- Selection of the fittest parents from the evaluated chromosomes of the population, and
- Evaluating each chromosome in the population using a fitness function.

A proper selection of the above operations does effect the performance of genetic algorithm. These three issues are dealt briefly in the subsections to follow.

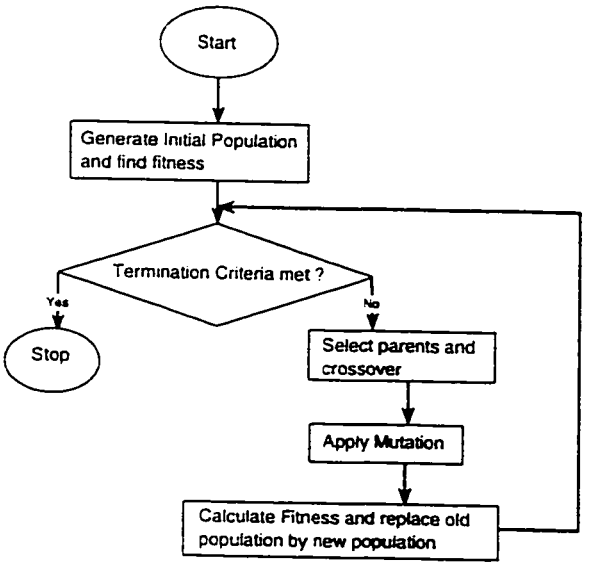

Figure 1.1: Block diagram of a simple Genetic algorithm

1.2.1 Genetic Operators

Reproduction, basically, involves the use of genetic operators on the strings of chromosomes. Some of the selected chromosomes are modified via genetic operators like crossover and mutation. Each genetic operator takes some chosen chromosomes (parents) and produces new chromosomes (offspring). The most common genetic operators include crossover and mutation.

Crossover Operator

Crossover operators combine sub-parts of two parent chromosomes to produce new children (offspring) thus allowing new points in search space to be tested. The operation of crossover starts with two parents independently selected at random from the population on the basis of their fitness. The selection is done in such a way that the better an individual's fitness, the more likely it is to be selected. The crossover operation produces two offspring. Each offspring contains some genetic material from each of its parents. One of the simplest ways of achieving this crossover is by partially exchanging a selection of strings between two random points. The main purpose of the crossover operator is to perform a wide spread search, exploring almost all the solution space. A lot of crossover operators have been designed in the recent past for solving combinatorial optimization problems.

Mutation Operator

Mutation is the secondary search operator which increases the variability of the population within the search space. The operation of mutation begins by randomly selecting a chromosome from the population. A mutation point along the string is chosen at random, and the single character at that point is randomly changed. The mutation operator offers the opportunity for new genetic material to be introduced into the population. Also, it is potentially useful in restoring genetic diversity that may be lost in a population. Because of premature convergence, mutation is used sparingly in most genetic algorithms work.

1.2.2 Parent Selection

Parent selection dynamics are based on an application-dependent measure of fitness called fitness function. The purpose of parent selection is to give more reproductive chances to those members of the population that are most fit. These selected chromosomes (called parents) are the fittest of the whole lot and so that they reproduce to bear children. One of the most widely used procedures for the above process is the roulette-wheel parent selection algorithm [4]. This algorithm is referred to as roulette-wheel because it can be viewed as allocating pie-shaped slices on a roulette-wheel to population members, with each slice proportional to the member's fitness. To reproduce, we spin the wheel, the selected member being the one in whose slice

the wheel ends up.

1.2.3 Fitness Function

The fitness function is the link between the genetic algorithm and the problem to be solved. It takes a chromosome as an input and returns a number, which is a measure of the chromosome's performance on the problem to be solved. Fitness function plays the same role in genetic algorithms as the environment plays in natural evolution. Usually, the fitness value is the value of the objective function or some scaled version of it. In general, the fitness function consists of the composition of two functions

$$u(x) = g(f(x)), \tag{1.1}$$

where f is the objective function and g transforms the value of the objective function to a non-negative number.

1.3 Literature Review

A lot of work has been done during the last few decades on null steering and its applications. Most of the research has been concentrated on the analytical development of null steering. We can broadly subdivide the research into two categories.

1. Analytical Null Steering Methods

2. Genetic Algorithm based Null Steering

1.3.1 Analytical Null Steering Methods

In a classic paper Schelkunoff [5] presented a method that is conducive to the synthesis of arrays whose patterns possess nulls in the desired directions. This method requires information of the number of nulls to be placed and their locations. The number of array elements needed, and their excitation values are then derived. Vu [6] described a method of null steering without using phase shifters. This is done by forcing the zeros of the array factor to occur in conjugate pairs on the unit circle in the complex plane. The paper also showed that if the number of jammers is much smaller than half the total number of elements in the array, it is possible to optimize the pattern as well as suppress the jammers.

Dawoud and Ismail [7] achieved null steering in an adaptive array by elemental position perturbations. An experimental verification of this technique was provided by them in [8]. They have suggested that null steering using element position perturbations is less complicated when compared to other existing techniques. Vu [9] in a paper that reviewed the principles and potential applications of null steering in phased arrays concluded that future research would be towards monolithic phased arrays with beam scanning and null steering likely to be achieved at low frequencies with the aid of high speed digital signal processors.

Dawoud [10] presented a methodology of null steering in scanned arrays by element

position perturbations. This method was devised to improve the performance of scanned arrays based on the null steering criterion, keeping beamwidth and side-lobe level variations to a minimum. Hu et al [11] in a recent publication proposed a synthesis method to design an array pattern with a deep null by controlling only the excitation phases of part elements by using a weight function to construct an objective function which was then minimized. Their results demonstrated the efficiency of this numerical method. Ko [12] investigated a fast null steering algorithm for adaptive arrays with a look direction constraint. In this, the LMS algorithm was used to adaptively adjust the positions of the array nulls one after another in a time multiplexed manner to track unknown jammers.

Nagesh and Vedavathy [13] have given a simple method to arrive at an optimum set of array excitations to achieve a specified radiation pattern. In this method, an auxiliary function is formulated based on the envelope of the required sidelobe structure and the array factor in the side lobe region. This function is minimized subject to the main lobe and null steering constraints to determine the excitations. Mismar and Ismail [14] used the Minimax approximation to steer the nulls of an array by controlling the current amplitudes. The technique determines the current amplitudes that produce the minimum sidelobe level for a given beam width and prescribed nulls in arbitrary directions. Wu [15] presented an iterative algorithm for obtaining a set of coefficients of a linear array that generate a desired main beam with suppressed sidelobe level. This technique can be applied to a linear array with

uniform or non-uniform spacing and isotropic or non-isotropic elements, and it also converges rapidly to the desired solution.

1.3.2 Null steering based on the Genetic Algorithm

In the last decade a lot of research has been done on the use of the Genetic Algorithm for array pattern synthesis and null steering. Dawoud et al [16] applied the genetic algorithm for null steering in adaptive arrays. They showed that using the GA it is possible to steer nulls precisely to the required interference directions and achieve any prescribed null depth. The paper also showed the potential of the GA for conformal array design.

Dawoud et al [3] made a comparison of the results obtained by using analytical methods for element position control, with the GA approach. They showed by using the GA for null steering, we get precise solutions to array adaptation as compared to the analytical method. A recent paper by Johnson et al [17] discusses the use of genetic algorithms for a variety of problems in electromagnetics such as design of shaped-beam antenna arrays, the design of broadband patch antennas etc. It concludes by emphasizing the suitability of the genetic algorithm for a broad class of electromagnetic problems. Marcano et al [18] applied the genetic algorithm for the synthesis of linear antenna arrays and concluded that the synthesis of the radiation pattern with many constraints is a non linear optimization problem, which is dif-

ficult to solve using methods based on deterministic rules because of local minima problems, and hence, they suggested the genetic algorithm as a solution.

Haupt [19] showed a method to optimally thin an array using genetic algorithms. The genetic algorithm determines which elements are to be turned off in a periodic array to yield the lowest maximum sidelobe level. Lu and Yan [20] applied the GA to synthesize the pattern for linear and curved arrays. They showed that the GA can be applied to synthesize arbitrary arrays which are difficult to be treated by other analytical or numerical methods.

Tennant et al [21] used the genetic algorithm for array pattern nulling by element position perturbation, and made comparisons with the results obtained from the analytical solution. This comparison showed some distinct advantages of using the genetic algorithm over analytical methods. Haupt [22] tried to overcome the large time consumption problem when arrays are numerically optimized, by a new method that ensures a fast convergence of the genetic algorithm. This is possible if the array parameters are encoded with a Gray code (Hamming distance =1) and therefore, are less likely to be disturbed during the crossover operation.

Johnson et al [23] discussed a number of applications of genetic algorithm such as design of light weight, broadband microwave absorbers, the reduction of array side-lobes in thinned arrays, the design of shaped beam antenna arrays etc. They concluded that the GA optimization is suitable for a broad class of problems related to aerospace antennas and electromagnetics.

In another recent publication Ares et al [24] used both simulated annealing and genetic algorithms to find optimum excitation for patterns with null filling. These methods have the advantage that the optimum aperture distribution is found without searching the entire solution space. A comparison between the performance of both methods shows that the GA's are faster than Simulated annealing for this problem. Chambers et al [25] applied the GA to the optimized design of radar absorbers for the end fire antenna array with both adaptive nulling and radiation pattern envelope limitations. The algorithms were robust and out-performed other optimization techniques such as Downhill Simplex and Simulated annealing.

Marcano et al [26] used the genetic algorithm to synthesize multiple beam linear antenna arrays with low sidelobe levels and stated that the results obtained showed the robustness of the GA.

1.3.3 Grating lobes and their suppression

Most of the work done on grating lobes and their suppression was in the field of Microwaves and Ultrasonics. Proukakis et al [27] discussed the ambiguities in uniform and non-uniform linear arrays. These ambiguities are viewed as the appearance of grating lobes when beam-forming is used.

Ragheb and Shafai [28] investigated a new concept in array design, where the level of the grating lobes is controlled by the Element pattern. Here, each array element operates in the first two modes TE_{11} and TE_{21} and the array pattern is shaped to

place a null in the direction of the grating lobes. This increases the inter-element spacing beyond that of normal arrays, without a serious pattern degradation due to the appearance of the grating lobes. Shafai [29] in a related paper dealt with enhancing the scan gain by element pattern synthesis. Scan gain can be achieved by moving the element pattern peak towards the scan angle. The grating lobes can be nullified by introducing an intentional null on the element pattern, at their location. Rew [30] also proposed a general scheme for eliminating all grating lobes in ultrasonic synthetic focusing using a linear array. Sharma and Calla [31] addressed the problem of the appearance of grating lobes in broad wall slotted waveguide array of shunt slots and presented an improved design technique to suppress these lobes. Lockwood et al [32] developed a method for designing sparse periodic arrays which avoided grating lobes by using different element spacings on transmission and reception. It was shown that using this technique the number of elements can be reduced at least four times with little degradation of the beam forming properties of the array.

1.4 Objectives of the Work

A survey of the literature showed that the appearance of grating lobes in scanned arrays results in a pattern that is ambiguous and hence not very useful [27]. We have also seen that the genetic algorithm has been applied to many array optimization

problems like null steering, pattern synthesis etc. [17], but no attempt has been made to use it for null steering to solve the grating lobe problem in scanned arrays. The solution to this problem opens many avenues that make arrays with large separation advantageous. Some of them are (i) Increased directivity, (ii) Increased scan range and, (iii) Simple feed network requirement for the antenna system. In our work that follows we intend to focus on the utilization of the genetic algorithm approach of null steering to tackle the problem of grating lobes.

In order to investigate scanned arrays and its patterns, we adopt the following line of research. At first, array factors for arrays with large separation d. (i.e $0.5\lambda < d < \lambda$) are analyzed. This is necessary to understand the radiation characteristics of such arrays precisely, some of which are array factor patterns and directivity. An interesting effect of scanning the main beam from broadside towards end-fire with large inter element spacing, is the appearance of the grating lobe in the pattern. An important part of the work is to use the genetic algorithm for null steering to reduce the grating lobe to a desired level, so as to have the new array factor pattern with increased directivity. For the purpose of null steering we use both the element position perturbations as well as complex weight perturbations. The algorithm developed for this work, has been coded using the C++ language, and plots generated using Matlab. A comparative study has been done for specific arrays on the change in directivity before and after grating lobe control. Grating lobe problem in Chebyshev arrays has also been studied. Radiation patterns generated

using the element pattern of a finite length dipole, are also studied in order to further control the side-lobes including grating lobes. In essence, this work concentrates on providing an effective solution to the problem of controlling grating lobe in scanned arrays.

Chapter 2

An Overview of linear arrays

2.1 Linear Arrays

An array of identical elements, all having uniform amplitudes of excitation and each with a progressive phase is referred to as an uniform array. An equi-spaced N element linear array is shown in figure 2.1.

Referring to the geometry of this figure, all elements have identical amplitudes of excitation, but each succeeding element has β progressive phase lead current excitation relative to the preceding one. The phase shift between two successive elements of this array is $[kdcos\theta]$ where k is the wave-number and is equal to $(2\pi)/\lambda$. Here, λ corresponds to the center frequency f, and d is the inter-element spacing. The direction pattern of the array, which is the relative sensitivity of response to signals from various directions may be found by considering the array factor term

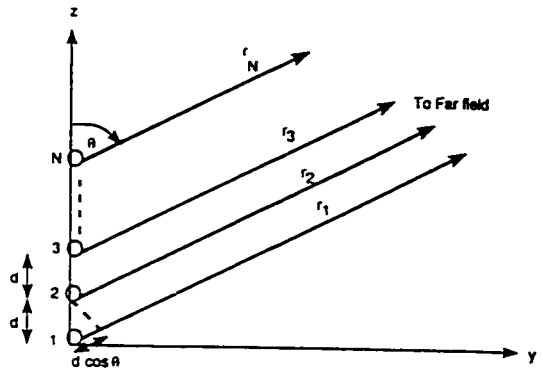

Figure 2.1: Far field geometry of N element array of isotropic sources positioned along the z-axis.

AF and it can be obtained by considering the elements to be point sources. It is given by: $AF = 1 + e^{j(kdcos\theta+\beta)} + e^{j2(kdcos\theta+\beta)} + ... + e^{j(N-1)(kdcos\theta+\beta)}$

The above expression can be simplified as:

$$AF = \sum_{n=1}^{N} e^{j(n-1)(kdcos\theta+\beta)} \tag{2.1}$$

Equation 2.1 can be written as

$$AF(\theta) = \sum_{n=1}^{N} a_n e^{j(n-1)\psi} \tag{2.2}$$

where $\psi = 2\pi dcos(\theta)/\lambda$. For the Scanned or Phased array $\psi = kd[cos\theta - cos\theta_0]$. Here, θ_0 is the main beam direction [1]. The total field for linear arrays is equal to the field of a single element positioned at the origin multiplied by the Array Factor (AF). This factored form of the expression is very useful, because the shape of the

element pattern is fixed, once the choice of elements for the array is made. Thus, in order to achieve a certain null configuration or a given pattern shape, the designer, in most cases, can utilize the expression of the array factor. A variation of the array design is by having uniform spacing and non-uniform amplitude of excitation. *Chebyshev* arrays and *Binomial* arrays are examples of this class of arrays.

2.1.1 Phased Arrays

Recent advances in high speed aircraft and missile technology have established the phased array antennas as an answer to radar systems [33]. This is due to the fact that phased arrays achieve beam steering electronically [9]. Maximum radiation can be oriented in any direction θ_0 by adjusting the phase excitation β between the elements to $\beta = -kdcos\theta_0$. Thus, by controlling the progressive phase difference between the elements, the main beam can be squinted in any direction to form a scanning array. Since in phased arrays the scanning must be continuous, the system should be capable of continuously varying the progressive phase between the elements. In practice, this is accomplished electronically by the use of ferrite phase shifters [1]. Implementation of a phased array system consists of two essentially independent tasks: determination of the current distribution on the array elements that is necessary to produce the desired radiation pattern, and implementation of an interconnection network which will generate the desired current distribution. Stuckman and Hill, [34] consider the first problem with particular emphasis on

achieving a type of radiation pattern particularly useful when the same antenna is used for transmission and reception.

2.2 Effects of Changing Array Parameters

A linear array has a number of parameters that contribute to its overall performance. Some of these important parameters are the number of elements 'N', and inter element spacing 'd'. When one or more of these parameters is varied, the performance of the array also changes. The following section analyzes these changes when either the number of elements or the inter-element spacing is varied.

1. **Fixing Spacing 'd' and increasing the number of elements 'N':** If this is done, the array length increases, implying an increased value of directivity and gain. But a complex feed network is required to feed the increasing number of elements.

2. **Keeping array length fixed:** In this case as N increases, d decreases, because the array length is fixed. The following results are observed:

   - No significant change in the main beam width.
   - Increased directivity
   - Higher mutual coupling, and hence a more complex feed network

3. **Fixing the number of elements and increasing the spacing d:** When N is kept constant, the array length increases by the increase in d. The following observations are made:

   - Narrow half power beamwidth (HPBW)
   - Higher directivity and gain
   - Less complex feed network

But as the inter-element spacing 'd' is increased well beyond 0.5λ ($d >> 0.5\lambda$) changes occur in the array factor pattern. High side-lobes resembling the main beam begin to appear. Their appearance causes a sudden reduction in the directivity of the array. These lobes, called **Grating Lobes**, tend to reduce the array directivity and gain . If the useful aspects of these large spaced arrays are retained and grating lobes controlled, then they become efficient and useful. Null steering using the Genetic algorithm is an important methodology that may prove useful in controlling the level of grating lobes. Figure 2.2 shows the antenna pattern for large inter element separation of 0.85λ when the main beam is scanned to $\theta = -30^0$ from the broadside (or 60^0). From this plot we note that a grating lobe shows up at 132^0 because of the combined effects of scanning the main beam to 60^0 and large inter-element spacing of 0.85λ.

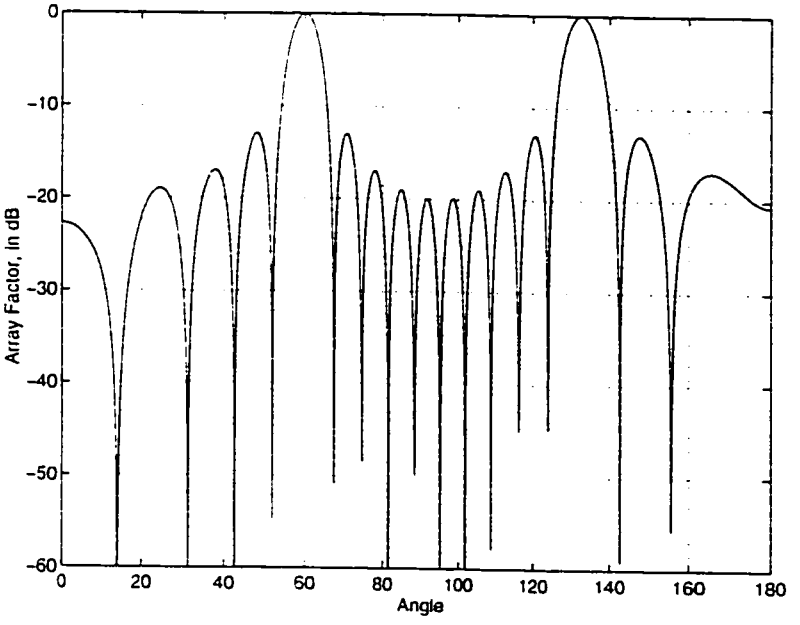

Figure 2.2: Pattern showing the appearance of a Grating lobe at 132^0 for a 10 element array with inter element separation d=0.85λ.

2.2.1 Grating Lobes

Only the lobe centered at beam steering angle u_0 is the desired lobe (main beam), and all additional lobes, of the same height as the main beam, are called grating lobes. Proper array design eliminates grating lobes by proper choice of dimensions or proper design of the antenna element or both [35]. For example, in a broadside array, the first grating lobe appears in the visible range when $d = \lambda$. Thus, a value of d smaller than one wavelength ensures that no grating lobe appears in the visible range of the pattern. In order to avoid grating lobes under all conditions of beam steering, the element spacing should satisfy the relation $d \leq \lambda/2$.

2.2.2 Effect of Grating Lobes on Directivity

The directivity of an array is determined entirely from its radiation pattern. It is defined as the ratio of the maximum radiation intensity u_{max} to the average radiation intensity u_{avg}. The directivity of a broadside array of isotropic elements having an inter-element separation $d = 0.5\lambda$ is equal to the number of elements N. Directivity curves (Directivity vs inter-element spacing) drop sharply near one and two wavelengths due to the emergence of grating lobes into the visible region. The directivity of a broadside array of isotropic elements is approximated by $D = 2L/\lambda$. This is a straight line approximation and it is accurate in the region from d slightly less than half wavelength to nearly one wavelength [36].

2.3 Appearance of grating lobes for a 10 element array

This section describes the the array factor of a 10 element uniform array, when the main beam is scanned to a direction θ_0 and the inter element spacing is varied from 0.5λ to 1.0λ. Figure 2.3 shows the comparison of grating lobe appearance angles for different main beam directions, with respect to inter element spacing. When the main beam is scanned to 85^0, the grating lobe appears when the inter element spacing d is about 0.92λ. This means that the pattern of this array is satisfactory,

until the spacing exceeds 0.9λ at which point grating lobes appear. Figure 2.3 also shows the useful range of this 10 element array for different main beam directions and spacings, for example, when the main beam is scanned to 30^0 a grating lobe appears for a spacing of 0.55λ.

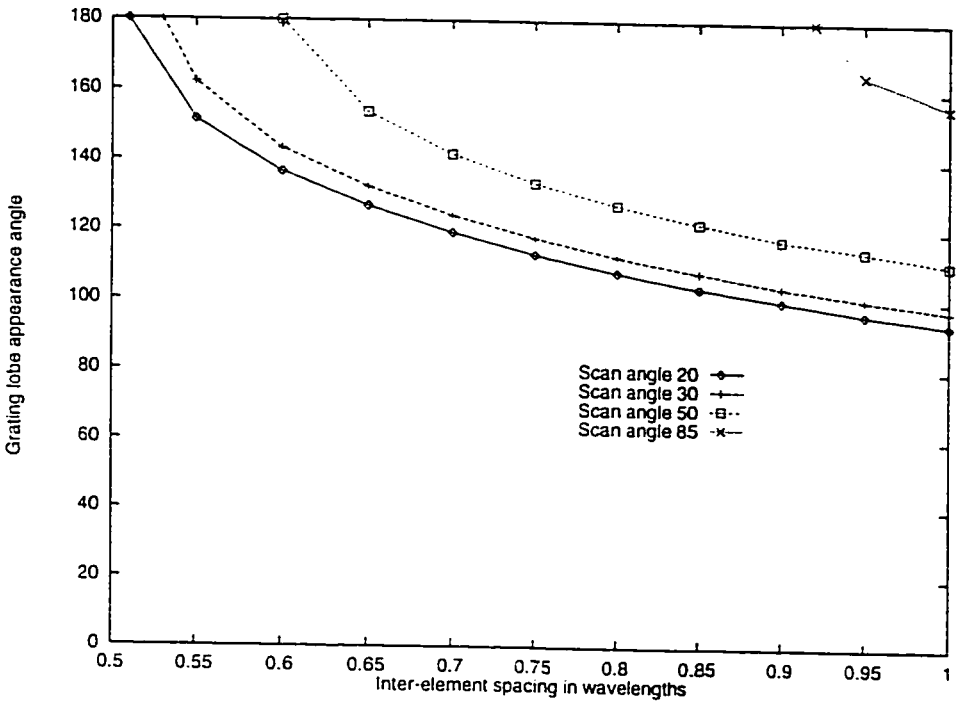

Figure 2.3: Plot showing the position of grating lobes for a 10 element array when main beam is directed to 20^0, 30^0, 50^0, and 85^0 .

2.4 Brief description of analytical null steering methods

2.4.1 Element position perturbations

A linear array of N equispaced, isotropic elements is considered which has the pattern

$$F(u) = \sum_{n=1}^{N} a_n e^{jd_n(u-u_s)} \tag{2.3}$$

and element positions of $d_n = d_0(n - N/2 - 0.5)$, where d_0 is the inter-element spacing and u_s is the main beam direction. Because the element position reference center is taken to be the center of the array, the element positions d_n have an odd symmetry with respect to the array reference center, i.e., $d_n = -d_{N-n+1}$; n=1,2,..., N

Null steering in linear arrays using element position perturbations is based on setting the array factor to zero in the directions of interfering sources while minimizing the perturbation in a mean square sense. The array factor of an N element array, when each element is located at d_n from the array centre and each position is perturbed Δ_n, is given by [7] and [8].

$$F(u) = \sum_{n=1}^{N} a_n e^{j(d_n+\Delta_n)(u-u_s)} \tag{2.4}$$

Assuming small perturbations, as given by equation 2.5

$$| \Delta_n(u - u_s) | << 1 \tag{2.5}$$

the Δ's can be obtained by linearizing and solving the array factor function as given by:

$$\sum_{n=1}^{N} a_n \Delta_n cos(d_n(u_m - u_s) = 0 \tag{2.6}$$

Complete analysis of this method is given in [7].

2.4.2 Complex weights

In this case both amplitude and element phase of the element weights can be perturbed fromtheir original values, the perturbed coefficients can be represented by

$$w_n = a_n + \Delta w_n \tag{2.7}$$

Here $\Delta w_n = a_n(\delta_n + j\phi_n)$. The first term on the RHS of equation 2.7 is the initial value of the n^{th} element weight a_n, and the second term is the perturbation of the weight. The perturbed array pattern is then

$$F(u) = \sum_{n=1}^{N} w_n e^{(jd_n(u-u_s))} \tag{2.8}$$

A detailed mathematical solution to equation 2.8 is provided by Styeskal [37].

2.5 Directivity calculation

For most practical antennas, radiation patterns are so complicated that their closed form mathematical expressions are unavailable. Even in those cases where mathematical expressions are available, integrating them to find the radiated power, which is necessary to compute the directivity, is not easy. Therefore alternate methods like usage of numerical techniques may be desirable. The use of numerical methods to perform complex mathematical operations can be done easily with high speed computers. In this work we have used the technique provided in [1] to calculate the directivity of the arrays.

To verify the accuracy of the developed routine for directivity calculation, we present the results for a 10 element array at broadside, whose inter-element spacing is varied from 0.1λ to 2.0λ. Figure 2.4 has been checked with the directivity plot available in the reference [36]and is in good agreement with it. From the plot we see that the directivity of the array falls suddenly when the spacing nears unity. This fall is due the appearance of grating lobes into the visible region.

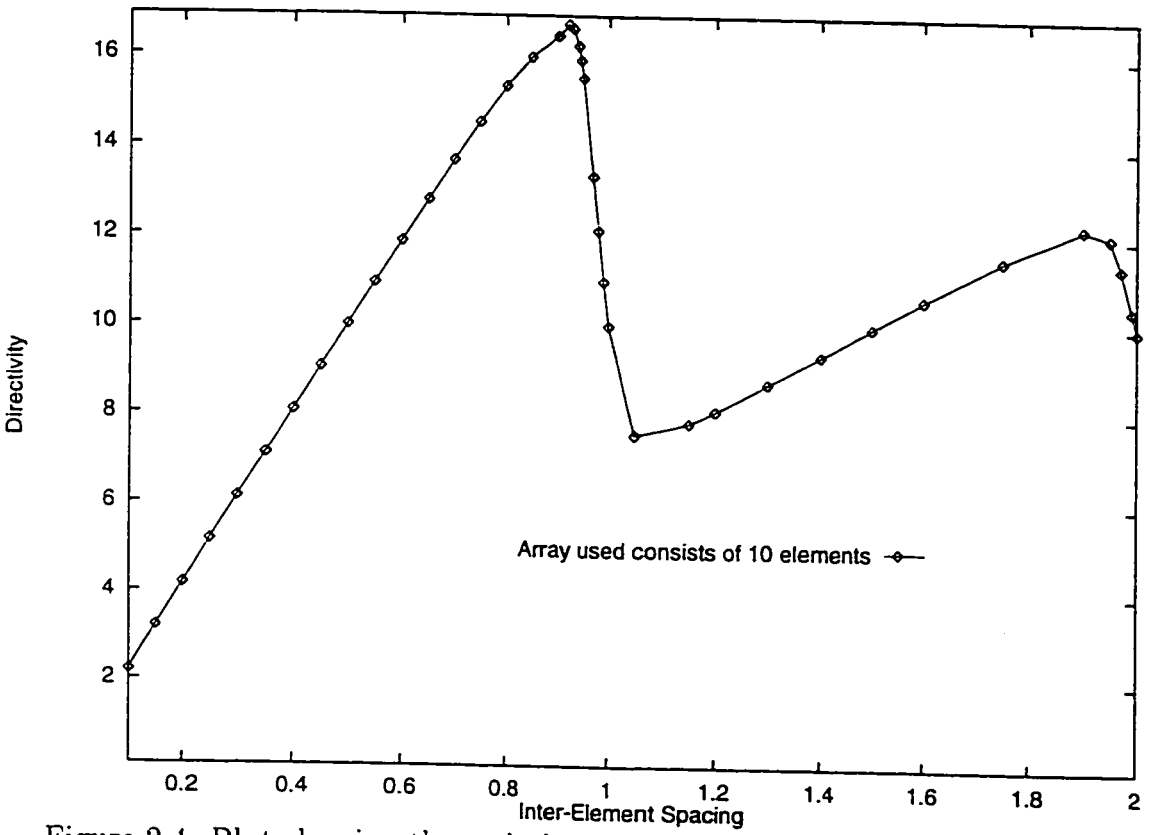

Figure 2.4: Plot showing the variation of directivity for a 10 element array.

Chapter 3

The genetic algorithm as applied to grating lobe control

3.1 Introduction

In this chapter, we provide a description of the software routines used for null steering using genetic algorithms for controlling grating lobes.

3.2 Program Description

We have divided the study of the developed routines into two sections. The first section describes the main algorithm and the next section describes each individual routine in detail. We describe the main program below.

Table 3.1: String representation

Elements	Chromosome string (position perturbations)
$N = 8$	-0.02 0.016 0.01 -0.09 -0.05 0.01 0.03 -0.07

The first step involved is the initialization of the program. Values of constants like the number of array elements 'N', the population size, the inter element spacing, etc, are initialized in the beginning. This parameter initialization is done in the "Initialize" routine. A set of chromosomes, which in our case are the perturbations, is generated randomly to form the initial population. It might be recalled that a chromosome is a *candidate solution* made up of units called *genes*, in our case each individual gene corresponds to the perturbation of that element. Chromosomes grouped judiciously into sets constitute a *population* and the population at a given stage is referred to as *generation*.

After generating an initial population, the "Calculate Fitness" routine is invoked to check the fitness of each chromosome in the population. In our case, fitness of a chromosome corresponds to the value of null depth in dB at the specified null position that is achieved with that chromosome . After sorting the population in descending order, the fitness of the best chromosome is compared with the required value of null depth. If this condition is not satisfied, the main loop of the program starts. An important consideration is to generate a new population from the old population and it is here that parent selection dynamics become important. Parent

chromosomes A and B are selected from the old population such that the probability of selecting a chromosome with higher fitness value is greater than that having a lower fitness value. The procedure used for the above process is the roulette-wheel parent selection algorithm. After selecting the parents A and B they are crossed over to generate a pair of children, this process being repeated for the whole population. Mutation is also performed based on a certain pre-set probability on a randomly selected gene of a chromosome. This important step not only helps the algorithm reach newer areas of the search space but also alleviates the local minima problem. The fitness of the new generation is calculated once again and chromosomes sorted in descending order based on their fitness. The fitness of the best chromosome is checked with the required null depth. If it is equal to or better than the required null depth the program stops and displays the successful chromosome, else the loop continues until it reaches a solution or exceeds a pre-defined number of generations. For more clarification, a flow chart of the adopted procedure is shown in figure 3.1.

3.3 Description of Routines

In this section each routine is described in detail. We start with the Initialization routine.

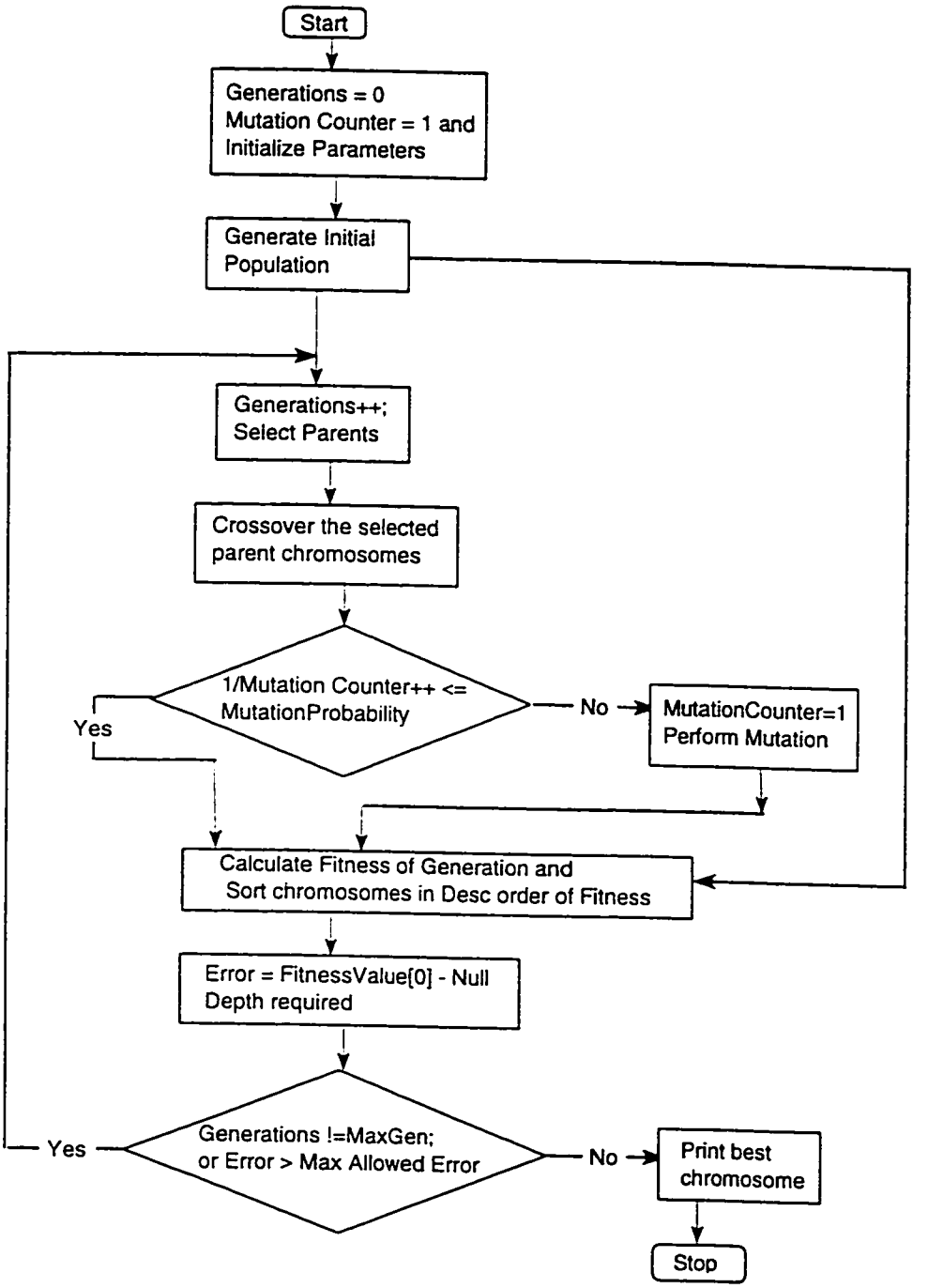

Figure 3.1: Flow chart of the Genetic algorithm as applied to the problem

3.3.1 Initialization

In this routine we define a few constants and also initialize the excitation amplitudes of the array elements, depending upon the type of the array (Uniform or Chebyshev). Values of important genetic algorithm parameters such as chromosome length, population size, and array parameters such as null positions, main beam direction, tolerance levels of perturbations, inter-element separation etc., are supplied to the program. This routine also calculates the element positions (D_n) based on the initial separation d_0 using the formula $D(n) = d_0(n - N/2 - 0.5)$. Here N is the number of elements and 'n' is the index.

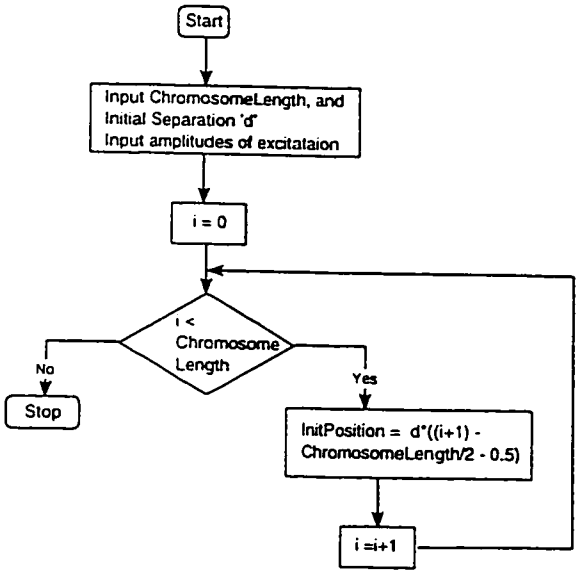

Figure 3.2: Flow chart of the Initialization routine

3.3.2 Generating Initial Population

In this routine we generate a set of chromosomes that form the initial population of prospective solutions. These are generated randomly. We have defined upper and lower bounds of tolerance for the perturbations. All genes of the chromosomes lie within this bound. This is done by the following formulation. $\Delta[i] = (LowerTolerence + rand() * (UpperTolerance - LowerTolerance))$. Here $rand()$ is a function that generates random numbers between 0 and 1.

3.3.3 Fitness Function

For array pattern nulling by element position control, the fitness function used is given in general terms by:

$$F = \frac{F(u_s)}{\Pi F(u_m)}. \tag{3.1}$$

where $F(u_m)$ is the value of the array factor at each of the desired null positions and $F(u_s)$ is the value in the main beam direction. Specifically, the formula of the array factor was used to calculate the fitness value when position perturbations were included. This is given by:

$$F(u) = \sum_{n=1}^{N} a_n e^{j(d_n + \Delta_n)(u_m - u_s)} \tag{3.2}$$

In the above equation Δ_n correspond to the position perturbations, u_s is the main beam direction and u_m is the null position. An advantage of using the GA is its ease of implementation without the use of mathematical assumptions when compared to the analytical method. Fitness values expressed in dB make the judgement of a chromosome's utility, easy.

Steering Two or more nulls

The formulation of the program changes slightly when two or more nulls are to be steered. For example if we wish to steer two nulls at $100^0$and 150^0 null steering is accomplished by working on the maximum of the two nulls. This procedure is described as follows. If the fitness value at 100^0 is $-25dB$ and that at that at 150^0 is $-30dB$ then the genetic algorithm works on the maximum of the two nulls i.e. the $-25dB$ deep null and tries to push it further down. After this operation suppose the depth of this null has changed from $-25dB$ to $-35dB$, then in the next step the GA works on the $-30dB$ deep null because it is the maximum of the two (i.e. $-30dB$ and $-35dB$) at this stage. This procedure continues until both steered nulls have the specified null depth. The same explanation holds for three nulls. Thus with a minor change in program steps, multiple nulls can be effectively steered. Figure 3.3 shows the flow chart of the fitness function evaluation.

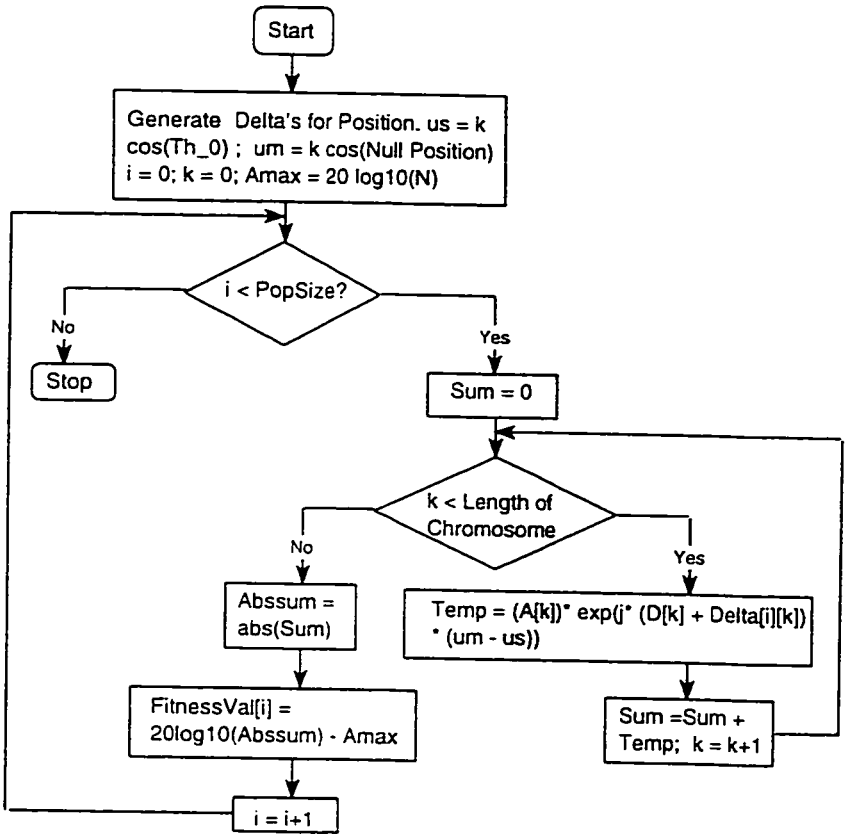

Figure 3.3: Flow chart showing the evaluation of Fitness Function

3.3.4 Parent Selection

For the purpose of parent selection we have used a popular stochastic selection strategy called *Roulette-wheel* selection. Here parents are selected based on a probability of selection given by the equation:

$$p_{selection} = \frac{Fitness(parent_i)}{\sum_i(parent_i))}. \tag{3.3}$$

The probability of selecting a parent from the population is purely a function of its relative fitness. Parents with high fitness will participate in the creation of the next generation more often than less-fit individuals. A good point of this mode of parent selection is that there is still a finite probability that highly unfit individuals will participate in at least some of the matings, thereby preserving their genetic information. Roulette wheel selection can be visualized as assigning a space on the wheel to members that is proportionate to their relative fitness. The wheel is "spun" and the member pointed to at the end of the spin is selected as a parent.

3.3.5 Crossover Operation

The crossover operator accepts the selected parents and generates two children. In the single point crossover shown in the flow chart of figure 3.5, a location that is in the middle of the parent chromosome is selected. The portion of the chromosome preceding the selected point is copied from parent number 1 to child number 1 and

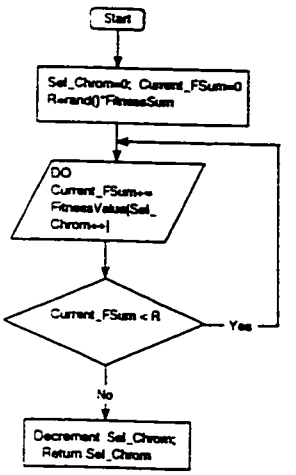

Figure 3.4: Flow chart showing the methodology for selecting parents

from parent number 2 to child number 2. The portion of the chromosome of parent number 1 following the randomly selected point is placed on the corresponding positions in the child number 2 and vice versa for the remaining portion of parent number 2's chromosome. The effect of crossover is to rearrange genes with the objective of producing better combinations, thereby resulting in fitter members. The crossover operator also helps in performing a wide spread search, exploring larger solution space.

3.3.6 Mutation Operation

The mutation operator provides for a change in the genetic makeup of the current population. In mutation, if $p > p_{mutation}$, an element in the string making up the chromosome, is randomly selected and changed. This is depicted in figure 3.6. Having a high rate of mutation results in a generation that may lose its genetic link

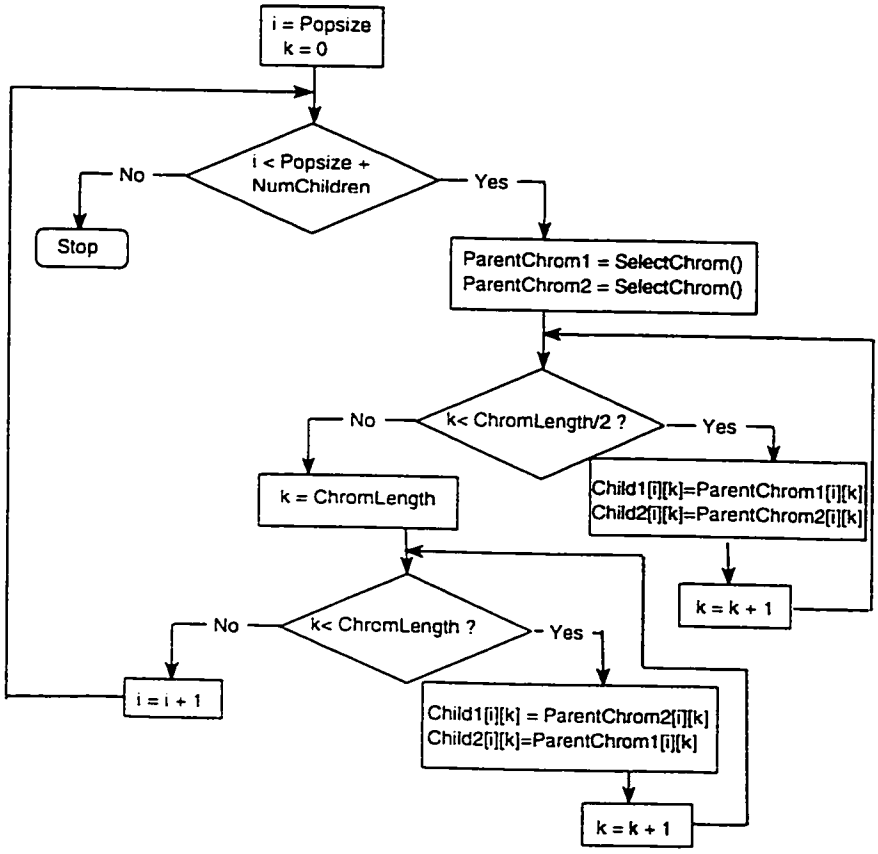

Figure 3.5: Flow chart showing the Crossover operation

due to excessive randomness. Hence, a low mutation probability was used, usually ranging from 0.01 to 0.1.

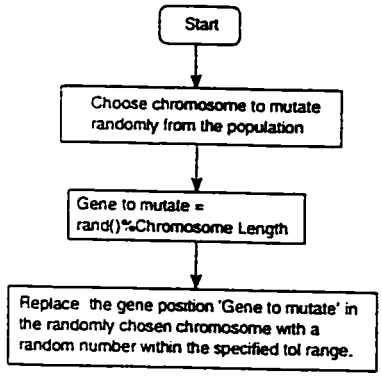

Figure 3.6: Flow chart showing the Mutation operation

3.3.7 Sorting of Chromosomes

After the calculation of fitness values in dB sorting is needed to find out the best chromosome in that generation. We have accomplished sorting using the "Selection Sort Algorithm" in which the first element of the array is compared with the second and swapping is done if the second is greater. This procedure is repeated by checking each element of the array with the first. Once this is done the first element of the array has the member with highest fitness. The procedure is repeated for the second, third, fourth elements and so on until all the elements of the array are covered and the array thus gets sorted in descending order. A flow chart of the procedure is given in figure 3.7.

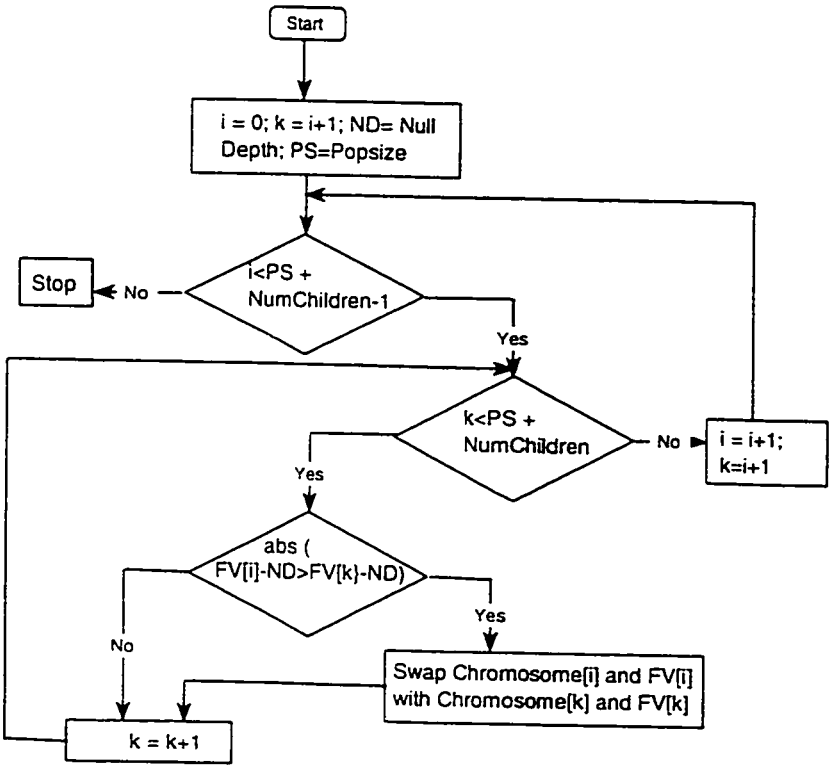

Figure 3.7: Flow chart showing the Sort operation

Chapter 4

Results and Discussion

In this chapter, we present and discuss the results achieved by applying grating lobe control on both uniform and non-uniform arrays. The benefit of applying genetic algorithm for null steering is also discussed. The organization of the results is as follows. At first, an array of 12 elements is considered. For this array the inter element separation 'd' is varied from 0.5λ to around 1.0λ, so that grating lobes appear, all through keeping the scan angle fixed. In order to control the grating lobe we use the genetic algorithm to steer nulls in its vicinity. The null depth chosen for the cases where the inter-element spacing is around 0.5λ is $-60dB$. For arrays with large inter-element spacing, the control level chosen was $-15dB$ to avoid pattern degradation by going for higher depths. For each case, we present the element position perturbations Δ_n of the elements that help achieve the required grating lobe control. Results are presented for a 20 element array, in order to show that this

algorithm can be applied to arrays of varying lengths. The $\Delta's$ for each case here are also provided. We also used the complex weight variations for grating lobe control and present results achieved using this technique in this chapter. Two or more nulls have been easily steered in different directions at the same time, as shown in this chapter. Results are also shown for three nulls steered in three different directions. We have also dealt with non-uniformly excited arrays namely Chebyshev arrays and have investigated the effects of grating lobe control on them.

4.1 Use of position perturbations

In this section the effect of perturbing the element positions on for null steering is studied. The set of position perturbations Δ_n's, are generated by the genetic algorithm and are used to find the new array factor pattern. Here, we analyse some of the plots obtained, and present the set of perturbations in tables, for each corresponding plot. The expression for the array factor that is used to generate these plots is given as:

$$F(u) = \sum_{n=1}^{N} (a_n)[(e^{j(d_n)(u-u_s)})(e^{j(\Delta_n)(u-u_s)})] \tag{4.1}$$

where Δ_n corresponds to the position perturbations. The other parameters in the equation are defined as: u_s is the main beam direction, a_n is the original amplitude and d_n is the position of the n^{th} element. In order to explain the concept of null

steering properly we present the case of a broadside array with a spacing of 0.5λ in figure 4.1. This is the simplest case considered for the 12 element array. Here, we have steered two nulls in different directions 140^0 and 160^0. The null depth chosen is $-60dB$ for both of them. The range provided for the perturbations was $\pm 0.07\lambda$ and the maximum number of generations provided for the algorithm to converge were 2000. The resultant pattern shown in solid lines depicts that both nulls were steered exactly to the specified positions and with the required depths. The population size chosen was 15 and the mutation rate chosen was 0.1. A small population size was chosen for achieving a faster convergence. The number of generations needed for convergence were 153. The position perturbations that produce these nulls is also provided in table 1.

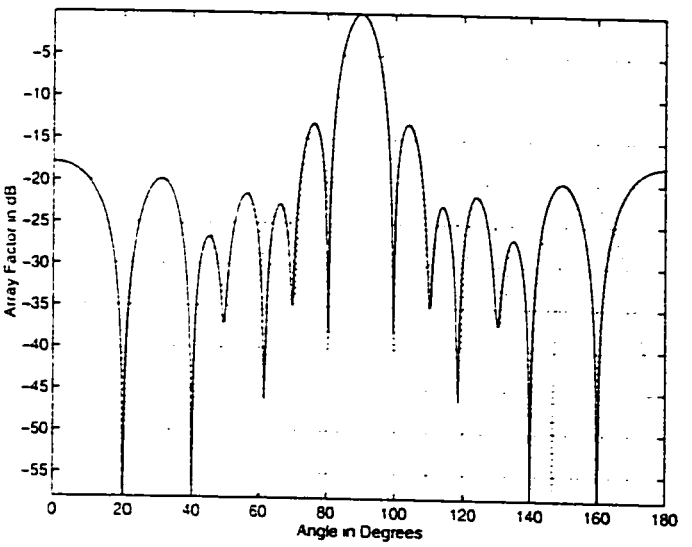

Figure 4.1: Array Factor Pattern for N=12, and separation=0.5λ with nulls imposed at 140^0 and 160^0. Dotted lines show the Original Pattern.

Table 4.1: Perturbations corresponding to Figure 4.1 in terms of λ

Perturbation Δ_D
-0.060894
0.047911
-0.022806
-0.027592
-0.059221
-0.063372
0.005496
0.024302
-0.037168
-0.046202
-0.063286
0.076061

4.1.1 Effects of increasing inter-element spacing with main beam at 70^0

In this section we analyze the effect of increasing the inter-element separation from 0.5λ to 0.8λ. The most important effect that large separations give rise to is the appearance of grating lobe. We have reduced its level to $-15dB$ or less, in order to make it just another side lobe by perturbing element positions. Because of its height and large beam-width the perturbations required for null steering need a higher tolerance range, mostly $\pm 15\%$ of the original positions as compared to that needed for a case where the spacing is 0.5λ, in which case the required range lies between $\pm 5\%$. Due to the increased range provided for the perturbations, the resultant pattern is a little disturbed as compared to the original. The pattern disturbance for the 0.5λ cases is negligible due to very small tolerance level provided for the perturbations. Figure 4.2 shows a simple case of a 0.5λ spaced 12 element scanned array (main beam at 70^0) with nulls steered to 140^0 and 160^0. These nulls are $-60dB$ deep and resultant pattern is close to the original. The number of generations needed were 167.

Figure 4.3 shows that by increasing the inter-element spacing to 0.6λ the level of the last side-lobe increases as compared to the previous case. A null is steered at 170^0 of depth $-60dB$ in order to control it. The number of generations needed were 506. Table 3 shows the perturbations, which are still around $\pm 5\%$. Due to

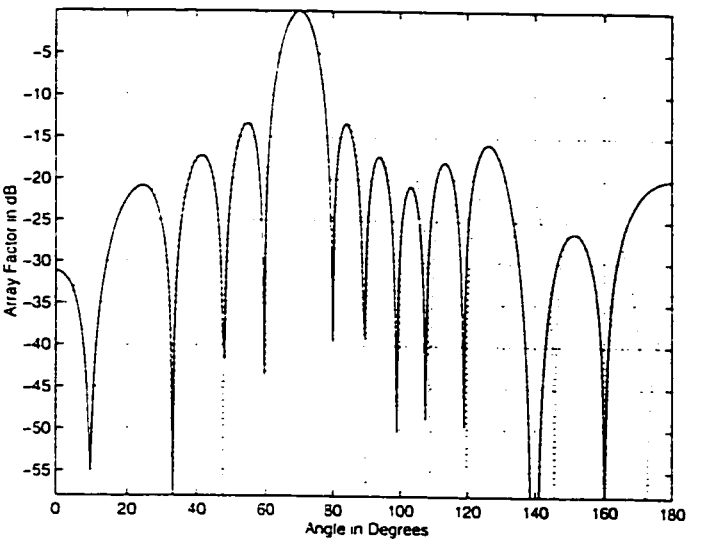

Figure 4.2: Array Factor Pattern for N=12, and separation=0.5λ with nulls imposed at 140^0 and 160^0 with main beam at 70^0. Dotted lines show the Original Pattern.

Table 4.2: Perturbations corresponding to Figure 4.2 in terms of λ

Perturbation Δ_D
-0.013677
-0.021996
0.029755
-0.029903
0.026078
-0.006084
-0.000301
-0.029678
0.029703
-0.029654
0.028975
0.020577

small perturbations, the resultant pattern is not disturbed and hence, close to the original. Figure 4.4 is an example of grating lobe control of a 12 element array

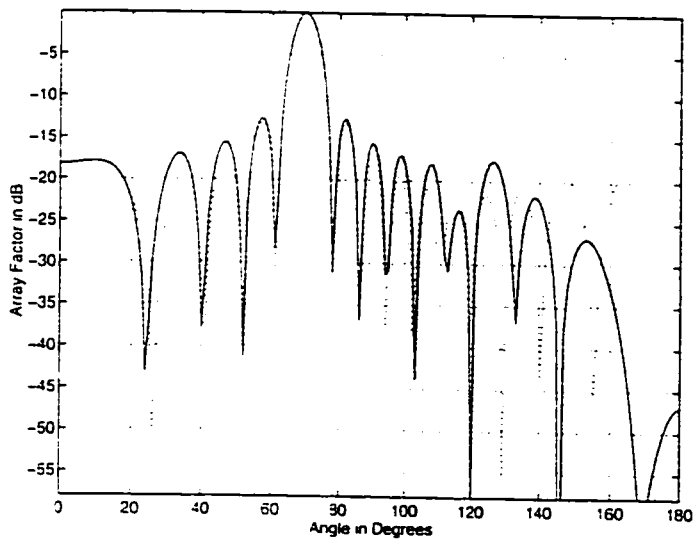

Figure 4.3: Array Factor Pattern for N=12, and separation=0.6λ with nulls imposed at 120^0 and 170^0. Control level specified is $-60dB$.

with a separation of 0.75λ using element position perturbations. The grating lobe level was constrained to $-15dB$ from the main beam maximum. It is seen here that controlling the grating lobe requires a larger tolerance range on perturbations (± 0.162) as compared to the case where the separation was 0.5λ. This is because it is difficult to control the grating lobe level with its large height ($0dB$) and wide beam-width, using a small solution space (tolerance level). The pattern is also slightly disturbed because of the relatively large perturbations used, as compared to the first case. The number of generations needed for convergence were 2589. Figure

Table 4.3: Perturbations corresponding to Figure 4.3 in terms of λ

Perturbation Δ_D
0.052670
-0.056661
-0.040925
-0.025198
-0.035490
-0.018464
-0.048671
0.001181
-0.027167
0.040669
0.035289
-0.043933

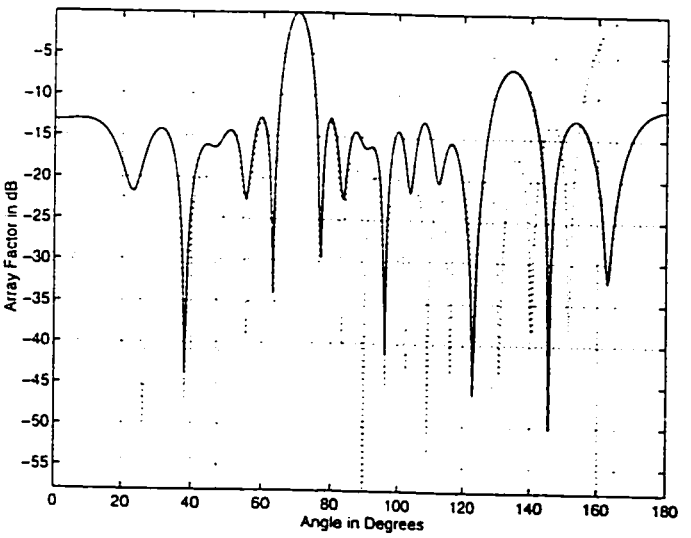

Figure 4.4: Array Factor Pattern for N=12, and separation=0.75λ with nulls imposed at 160^0 and 170^0. Control level specified is $-15dB$.

4.5 shows that an increase in the element spacing to 0.8λ shifts the position of the peak of the grating lobe to 155^0. Hence grating lobe control was employed with a control depth of $-15dB$ at the specified directions of 150^0 and 160^0, but in the resultant pattern, one side-lobe with its peak at 140^0 has a level of $-7dB$, thereby showing little improvement when compared to the original pattern. The number of generations needed were 4565.

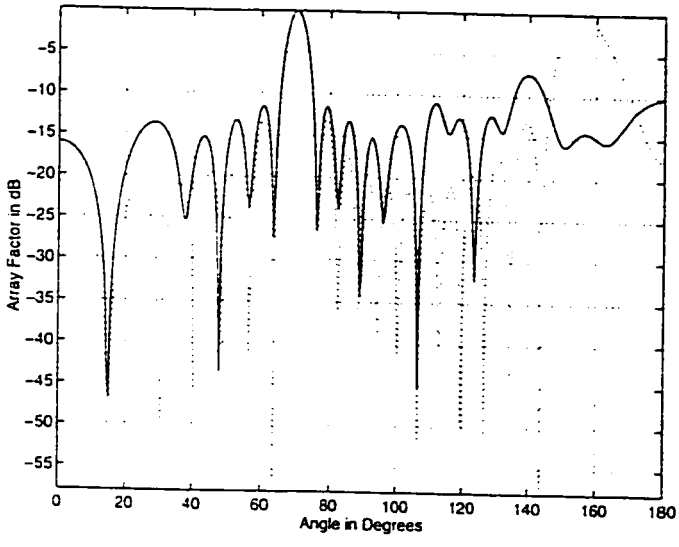

Figure 4.5: Array Factor Pattern for N=12, and separation=0.8λ with nulls imposed at 150^0 and 160^0. Control level specified is $-15dB$.

4.1.2 Main beam at 20^0

In this section we show an example of the main beam being scanned to 20^0. If we steer the main beam thus far, even for small element separations, we see the appearance of grating lobe. Figure 4.6 shows the pattern of this array where elements

Table 4.4: Perturbations corresponding to Figure 4.4 in terms of λ

Perturbation Δ_D
0.160199
0.161352
0.161451
-0.161165
-0.160228
0.161352
0.161352
-0.161224
-0.160761
-0.161185
0.160475
-0.161254

Table 4.5: Perturbations corresponding to Figure 4.5 in terms of λ

Perturbation Δ_D
0.174515
-0.174483
-0.176957
-0.176427
0.174818
0.176838
0.176838
0.175336
-0.175725
0.176103
-0.175034
-0.176255

have a spacing of 0.5λ. The level of the last side lobe in the unperturbed pattern is too high, and to control it we have placed a null at 170^0. Also, to control any other side lobe from rising much in other directions, we have placed a null at 120^0 also. The number of generations needed were 1800.

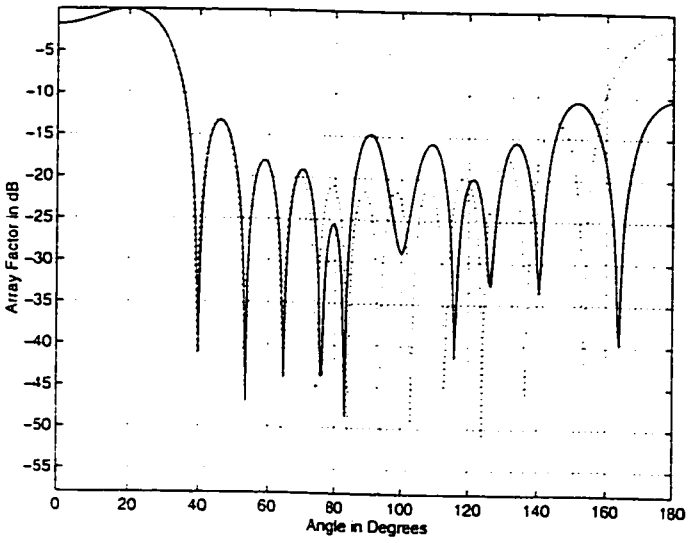

Figure 4.6: Array Factor Pattern for N=12, and separation=0.5λ with nulls imposed at 145^0 and 170^0 with main beam at 20^0. Dotted lines show the Original Pattern.

4.2 Application to 20 and 32 element arrays

In this section we apply this method by to a 20 element array whose main beam is scanned to 60^0. The inter element spacing chosen is 0.75λ. Due to the large scan angle and spacing a grating lobe appears with its peak at 146.4^0. The half power beamwidth for this lobe is 6.2^0 as compared to 3.9^0 of the main beam. In

order to bring its level down we have controlled side lobes at 144^0 and 148^0. The resultant pattern is disturbed. The mutation probability employed was 0.1 and the population size chosen was 15. 8166 generations were needed for the algorithm to converge to the required specifications. Figure 4.7 shows these details. The plot in

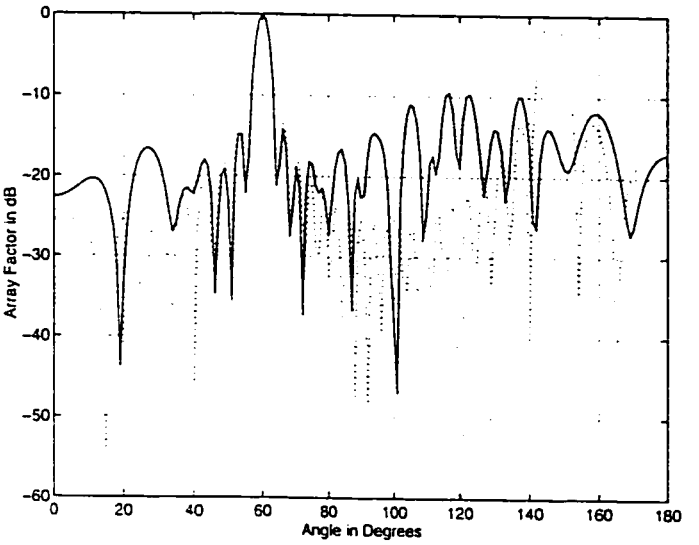

Figure 4.7: Array Factor Pattern for N=20, and separation=0.75λ with nulls imposed at 144^0 and 148^0 with main beam at 60^O. Dotted lines show the Original Pattern.

figure 4.8 refers to a 32 element array whose main beam is scanned to 60^0 and has an inter-element spacing of 0.75λ. The peak of the grating lobe is at 146.4^0 and hence two nulls of depth $-15dB$ were steered at 145^0 and 147^0, thereby bringing its level down. The number of generations needed were 13210. From the last two examples of 20 and 32 elements we can conclude that application of null steering using the genetic algorithm can be performed for arrays with any number of elements.

Table 4.6: Perturbations corresponding to Figure 4.6 in terms of λ

Perturbation Δ_D
0.067950
0.067975
0.067975
0.034734
0.064111
-0.049812
0.045089
-0.051269
-0.018443
-0.067846
-0.067622
-0.067859

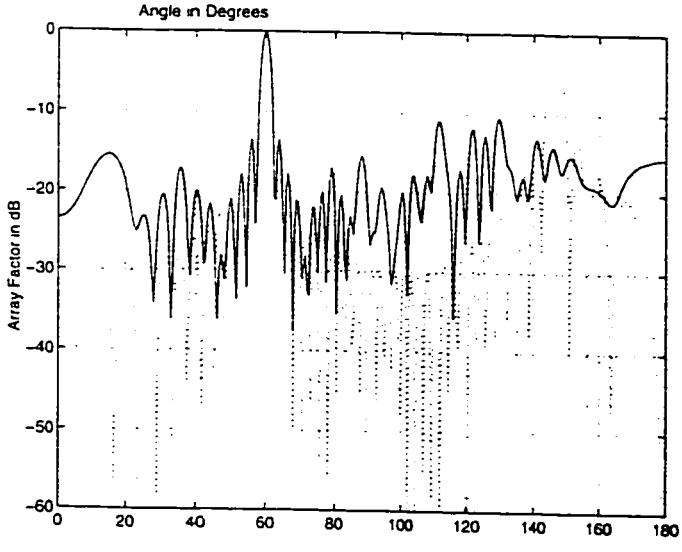

Figure 4.8: Array Factor Pattern for N=32, and separation=0.75λ with nulls imposed at 145^0 and 147^0 with main beam at 60^O. Dotted lines show the Original Pattern.

Table 4.7: Perturbations corresponding to Figure 4.7 in terms of λ

Perturbation Δ_D
-0.164480
-0.168890
0.160890
0.163494
-0.162456
0.167914
0.158721
0.154321
-0.170000
-0.169689
0.169689
-0.169533
0.140293
-0.168993
-0.167406
-0.168454
0.167126
0.165445
-0.168454
0.163670

4.3 Complex Weight perturbations

The versatility of the genetic algorithm, vis-a-vis usage of any method of perturbation to steer nulls is validated by the use of the amplitude-phase type of perturbations, also known as complex weight perturbations. The set of amplitude perturbations Δ_{an}'s, and phase perturbations Δ_{pn}'s , are generated by the genetic algorithm and are used to find the new array factor pattern.In this section we analyse some of obtained patterns, and present the set of perturbations in tables, for each corresponding pattern.

Figure 4.9 shows the application of null steering using complex weight perturbations to a 12 element uniform array. The array is broadside, and nulls of depth $-60dB$ are steered at 140^0 and 160^0. The number of generations required to achieve this objective are 294. Mutation rate chosen is 0.1 and population size chosen was 15. Figure 4.10 refers to the 12 element scanned array (main beam at 50^0) , 0.5λ spaced, and where nulls are placed in the directions 115^0 and 160^0 to control side lobes. These examples show the ease of placing nulls with the complex weight technique.

Investigation of the effect of scanning the main beam towards 0^0 showed that the grating lobe appears for values of spacing as small as 0.5λ. Figure 4.11 proves that when the main beam scanned to 0^0 with a spacing of 0.5λ a grating lobe appears. In order to bring it to an acceptable level, we have steered two nulls at 170^0 and 180^0

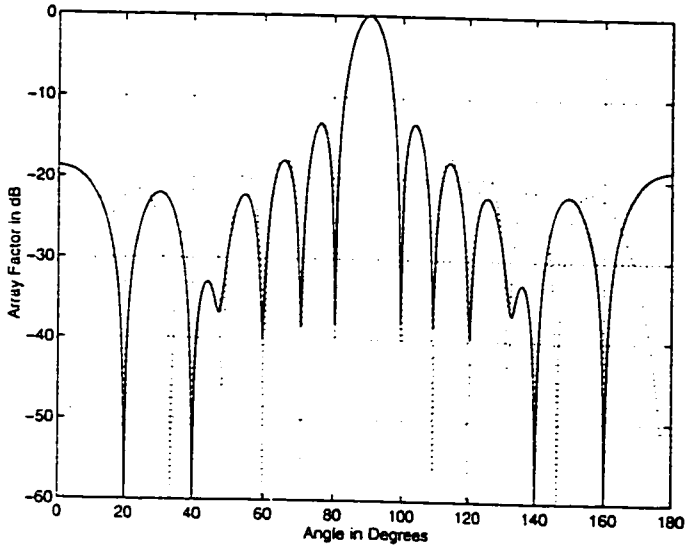

Figure 4.9: Array Factor Pattern for N=12, and separation=0.5λ with nulls imposed at 140^0 and 160^0. Dotted lines show the Original Pattern.

Table 4.8: Perturbations corresponding to Figure 4.9

Perturbation Δ_{pn}	Amplitude Perturbation Δ_A
-0.042547	-0.017510
0.038488	0.017513
-0.008165	0.005814
0.013103	-0.014946
-0.014870	0.019045
-0.015850	-0.009917
-0.011077	-0.012181
-0.029977	0.008433
-0.011083	0.017714
0.049579	0.008145
-0.046771	0.018339
0.033181	-0.019856

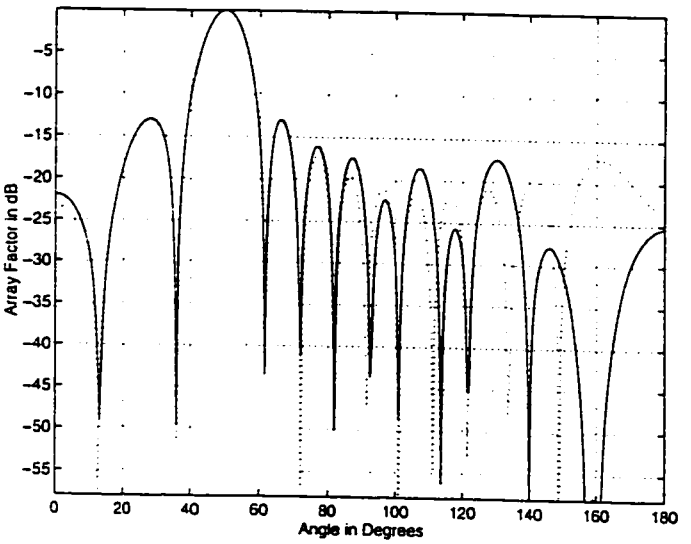

Figure 4.10: Array Factor Pattern for N=12, and separation=0.5λ with nulls imposed at 115^0, 140^0 and 160^0 with main beam at 50^0. Dotted lines show the Original Pattern.

Table 4.9: Perturbations corresponding to Figure 4.10

Perturbation Δ_{pn}	Amplitude Perturbation Δ_A
0.027467	-0.019873
-0.027745	-0.019916
-0.027988	0.019821
0.009337	0.019741
0.025908	0.012389
-0.019181	-0.009110
0.017563	-0.019485
-0.026816	-0.017454
-0.007476	0.019988
0.027188	0.019960
0.027600	-0.018937
-0.027856	-0.019926

in 8343 generations. The resultant pattern is disturbed as compared to the original.

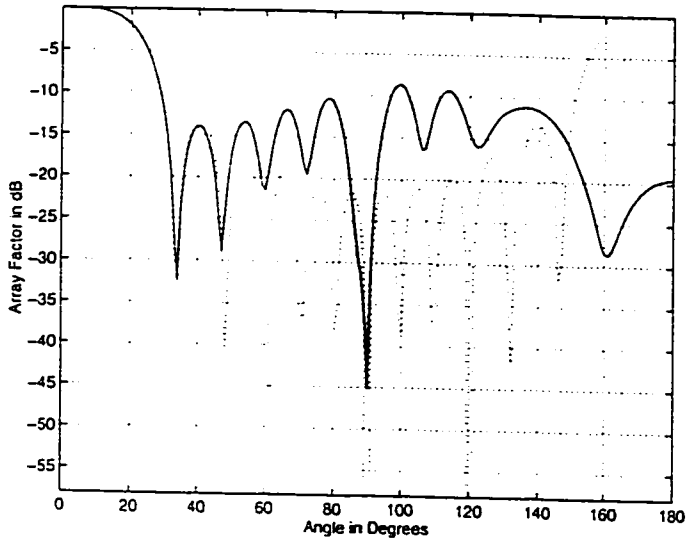

Figure 4.11: Array Factor Pattern for N=12, and separation=0.5λ with grating lobe control at 170^0 and 180^0 for the end-fire array. Dotted lines show the original pattern.

4.3.1 Main beam at 60^0

Figures 4.12 and 4.13 correspond to the 12 element array whose main beam is scanned to 60^0. For a spacing of 0.68λ, it is seen from figure 4.13 that the grating lobe appears and three nulls were steered to control it in 9879 generations. Grating lobe control using complex weights is achieved at specified directions, but the resultant pattern has some side lobes that have a higher level when compared to the original.

Table 4.10: Perturbations corresponding to Figure 4.11

Perturbation Δ_{pn}	Amplitude Perturbation Δ_A
0.108010	-0.085732
-0.118227	-0.082562
-0.119114	-0.088055
0.118118	-0.084001
0.113320	-0.081694
0.113935	-0.086902
-0.118579	-0.088292
0.118828	-0.085770
-0.119648	-0.087347
-0.111394	-0.080848
0.119648	-0.084402
-0.119802	-0.080249

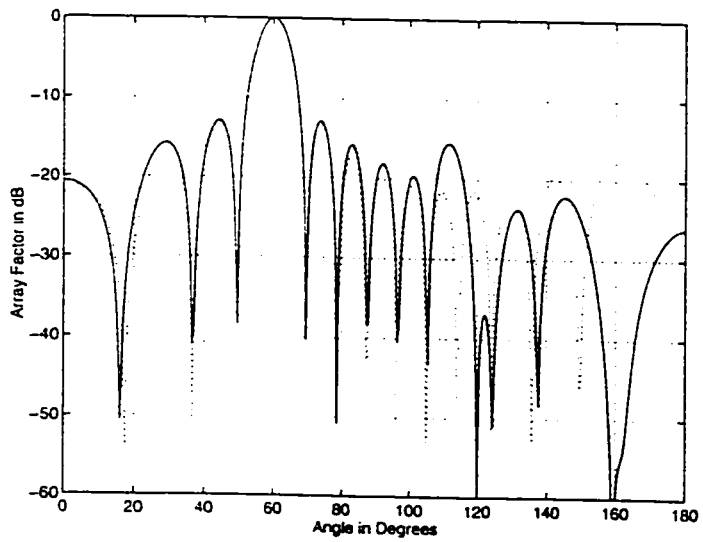

Figure 4.12: Array Factor Pattern for N=12, and separation=0.55λ with nulls of depth $-60dB$ imposed at 120^0 and 160^0 . Dotted lines show the Original Pattern.

Table 4.11: Perturbations corresponding to Figure 4.12

Perturbation Δ_{pn}	Amplitude Perturbation Δ_A
0.034787	-0.024841
-0.033867	0.023051
-0.006532	-0.021751
-0.028921	0.024962
0.039622	0.014453
-0.015549	-0.020763
0.011217	-0.023633
-0.038757	0.022607
0.024653	0.024985
0.010609	-0.024797
0.037476	0.022606
-0.039795	-0.024275

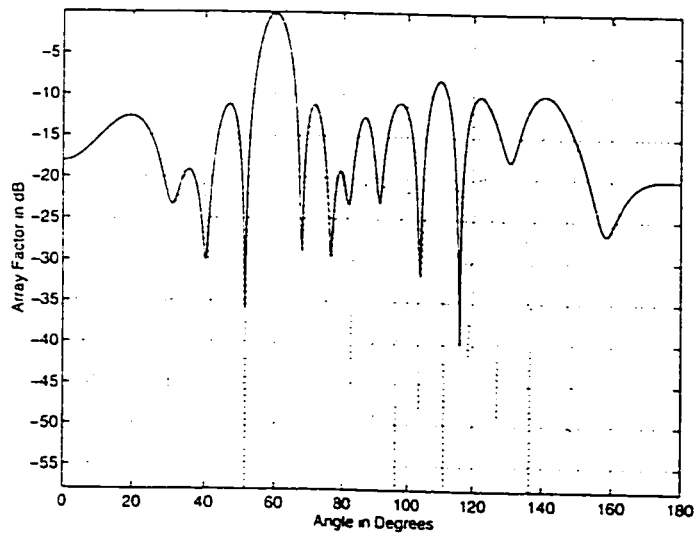

Figure 4.13: Array Factor Pattern for N=12, and separation=0.68λ with lobe control imposed at 155^0, 170^0 and 180^0 with main beam at 60^0. Dotted lines show the Original Pattern.

4.3.2 Main beam at 70^0

Figure 4.14 shows an array factor pattern generated for a 12 element array with an element spacing of 0.6λ with main beam at 70^0. It is seen here that the side-lobe farthest from the main beam starts to get higher. We have steered a null in that direction i.e at 160^0 to bring its level down. The tolerance range that was provided for the amplitude perturbations was $\pm 2\%$ and that for the $\Delta'_{pn}s$ was $\pm 3\%$. The number of generations needed for the program to converge to the above specifications were 3632.

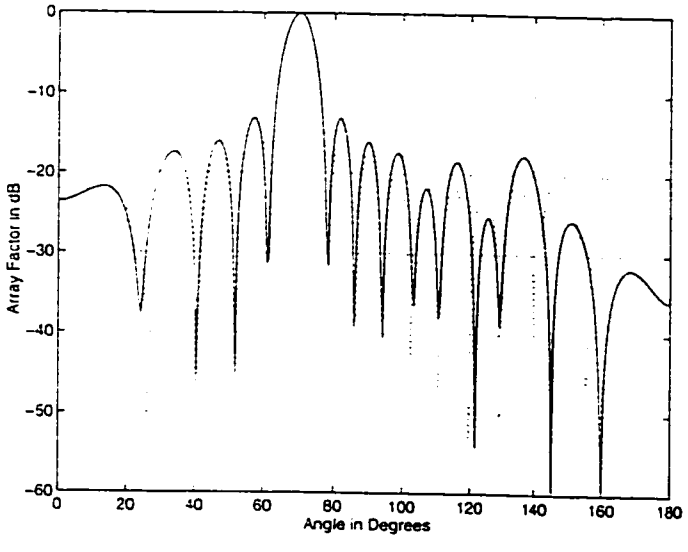

Figure 4.14: Array Factor Pattern for N=12, and separation=0.6λ with lobe control imposed at 145^0 and 160^0 with main beam at 70^0. Dotted lines show the original pattern.

The plot in figure 4.15 shows the control of grating lobe when this 12 element array has a spacing of 0.75λ using complex weight perturbations. The number of

Table 4.12: Perturbations corresponding to Figure 4.13

Perturbation Δ_{pn}	Amplitude Perturbation Δ_A
0.152552	-0.066783
0.158776	-0.067321
-0.163731	0.066992
0.163157	-0.069791
-0.163409	0.064651
-0.161807	-0.067501
-0.159763	-0.062677
0.163932	0.068992
0.163630	0.057148
-0.159602	-0.068193
0.159652	0.068624
-0.157165	-0.067180

Table 4.13: Perturbations corresponding to Figure 4.14

Perturbation Δ_{pn}	Amplitude Perturbation Δ_A
0.029429	-0.011423
-0.026226	-0.019916
-0.026409	0.019821
-0.003665	0.013785
0.027275	-0.007793
-0.028326	0.015596
0.014408	-0.014806
-0.027365	0.019468
-0.017235	0.019709
0.029747	-0.017528
0.027702	-0.019443
-0.029059	0.019183

generations needed here for convergence are 9688.

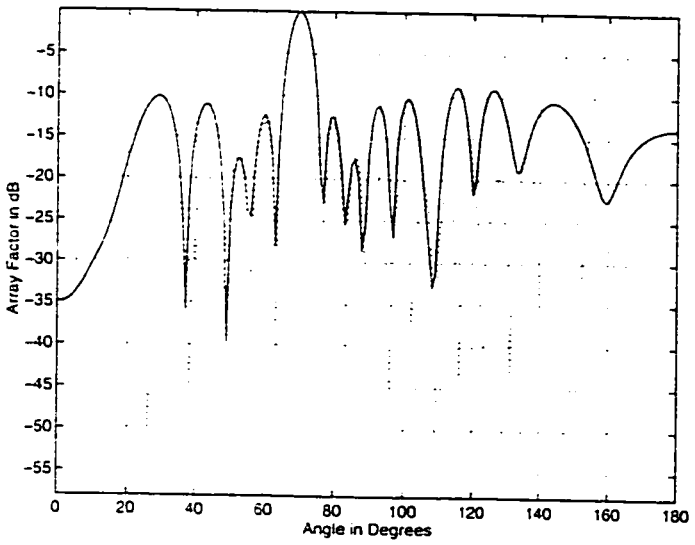

Figure 4.15: Array Factor Pattern for N=12, and separation=0.75λ with nulls imposed at 160^0 and 170^0 with main beam at 70^0. Dotted lines show the Original Pattern.

Table 4.14: Perturbations corresponding to Figure 4.15

Perturbation Δ_{pn}	Amplitude Perturbation Δ_A
0.164637	0.098035
-0.164557	-0.099652
0.165000	0.098669
0.164899	0.099554
-0.163258	-0.099829
-0.164930	-0.099786
-0.164658	0.084277
0.164366	-0.099908
-0.164577	0.099432
0.164859	-0.099182
0.163530	-0.097009
-0.164758	0.099164

4.3.3 Application to a 20 element array

Using complex weight perturbations, a 20 element scanned array's grating lobe is controlled as shown by figure 4.16. The main beam is at 80^0 and the elements have a spacing of 0.85λ between them. The grating lobe is controlled at 172^0 in 5140 generations.

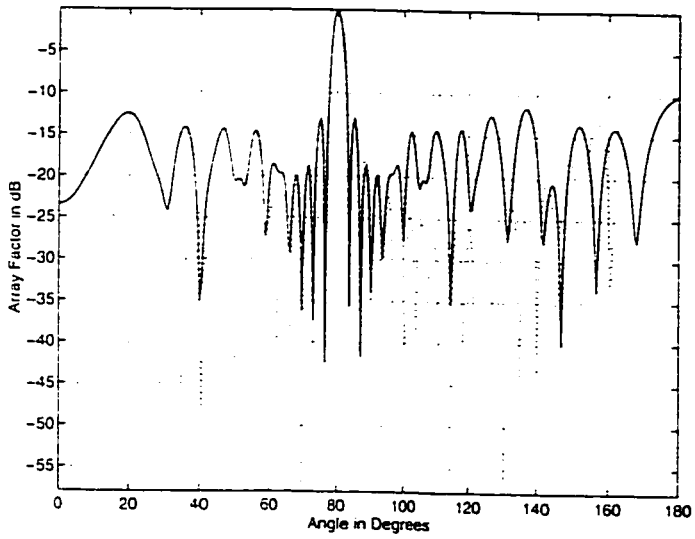

Figure 4.16: Array Factor Pattern for N=20, and separation=0.85λ with lobes controlled at 140^0, 160^0 and 172^0 with main beam at 80^0. Control level chosen is $-15dB$. Dotted lines show the Original Pattern.

4.4 Application to Chebyshev arrays

The Dolph-Chebyshev method, used in the implementation of the Chebyshev array, has many practical applications. This method was originally introduced by Dolph

Table 4.15: Perturbations corresponding to Figure 4.16

Perturbation Δ_{pn}	Amplitude Perturbation Δ_A
0.155719	0.098547
-0.160196	-0.088513
0.180827	0.006125
0.179737	0.026243
0.173776	-0.000821
-0.161924	0.075079
0.173741	-0.097217
0.137036	-0.024381
-0.190000	0.036918
0.140202	-0.066082
-0.142754	0.016892
0.169380	-0.043632
0.155035	-0.013114
-0.133406	0.014158
-0.164081	-0.042790
0.178426	-0.092138
-0.129197	-0.086413
-0.186683	-0.010062
-0.186347	-0.088861
-0.179400	0.024406

and investigated afterwards by Riblet et al. The element amplitude excitation coefficients of this array are related to Chebyshev polynomials. All the side lobes of a Dolph-Chebyshev array pattern have equal height. There is a relation between cosine functions and Chebyshev polynomials. For example the Chebyshev polynomial $T_3(z) = 4z^3 - 3z$ is equal to the cosine function $cos(3z) = 4cos^3(z) - 3cos(z)$. The recursive formula for Chebyshev polynomials is given by $T_m(z) = 2zT_{m-1}(z) - T_{m-2}(z)$. We know that the array factor is a summation of cosine terms whose form is same as Chebyshev polynomials. The unknown amplitude coefficients of the array factor can be determined by equating the series representing the cosine terms to the appropriate Chebyshev polynomial. The order of the polynomial should be one less than the total number of elements of the array.

Ares et al [38] presented a new algorithm for calculating the excitation coefficients of Dolph-Chebyshev arrays based on reconstructing the Schelkunoff polynomial from its roots. In this work, we have used the design procedure provided in [1] and designed a 20 element array with a side lobe level of -18dB. The normalized coefficients of excitation of this array were [0.620, 0.614, 0.684, 0.665, 0.629, 0.582, 0.525, 0.462, 0.396, 1.0]. Both element positions and complex weight perturbations were applied for controlling grating lobes. Here, we present an example using complex weight perturbations in figure 4.17 for the 20 element broadside array with an element separation 0.5λ with nulls steered to 145^0 and 160^0 in 3956 generations. Figure 4.18 has been generated using the element position perturbations for the same null positions.

The number of generations needed were 2696. The table of perturbations that is used is also provided with each plot.

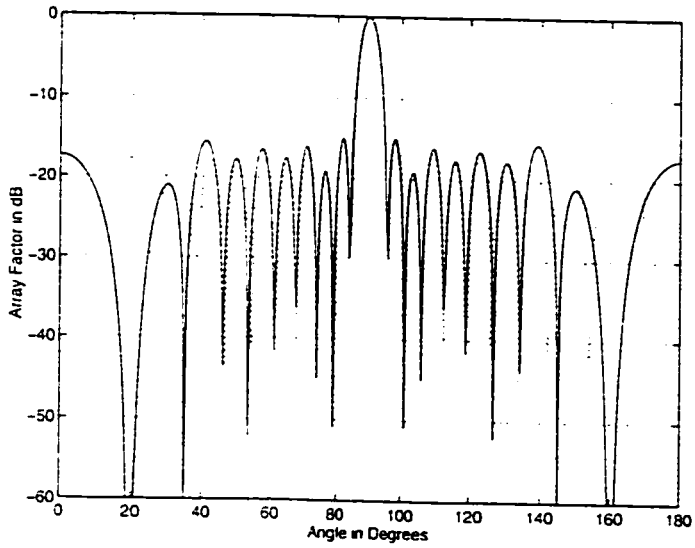

Figure 4.17: Array Factor Pattern for N=20, and separation=0.5λ with nulls imposed using complex weight perturbations at 145^0 and 160^0 with main beam at 90^0 and Control level chosen is $-60dB$.

Figures 4.19 and 4.20 are related to the Chebyshev array of 0.85λ spacing and whose main beam is at 80^0. Figure 4.19 shows the resultant pattern when position perturbations are used for grating lobe control, while figure 4.20 shows the pattern that results when complex weights are used. These plots show that the resultant patterns are a little disturbed as compared to the original. The number of generations needed were 14206 and 19800 respectively.

Table 4.16: Perturbations corresponding to Chebyshev Figure 4.17

Perturbation Δ_{pn}	Amplitude Perturbation Δ_A
0.045959	-0.009811
0.000145	0.009412
-0.046078	-0.009609
0.040783	0.009351
-0.048910	0.005688
0.047821	-0.001463
-0.043524	0.009393
0.048962	-0.003742
-0.032269	0.009517
-0.034219	-0.007789
-0.018188	-0.008951
0.036206	0.006557
-0.034326	-0.009368
0.048914	0.008712
-0.048202	0.008526
0.044217	-0.007753
-0.044443	0.009584
0.049634	-0.009557
-0.012618	0.009944
-0.045941	-0.009468

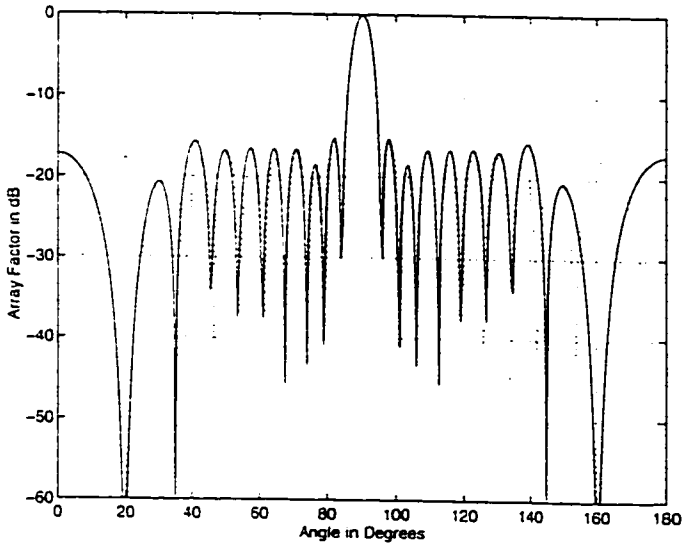

Figure 4.18: Array Factor Pattern for N=20, and separation=0.5λ with nulls imposed using position perturbations at 145^0 and 160^0 with main beam at 90^0 and Null depth chosen is $-60dB$.

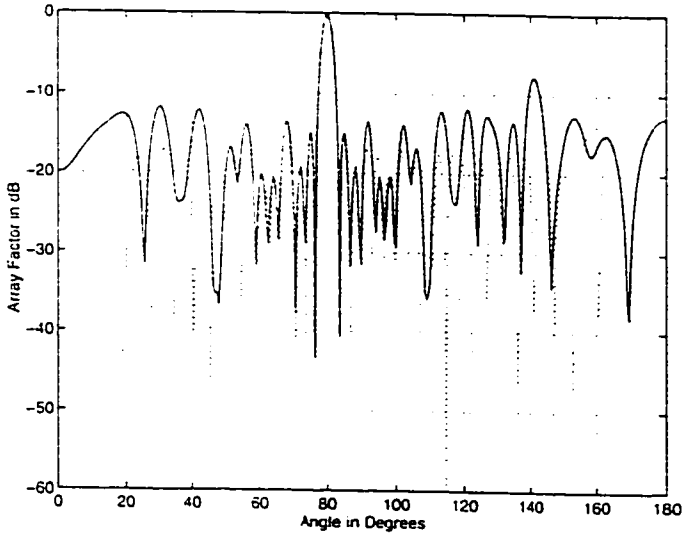

Figure 4.19: Array Factor Pattern for N=20, and separation=0.85λ with nulls imposed using position perturbations at 165^0 and 175^0 with main beam at 80^0 and Control level chosen is $-15dB$.

Table 4.17: Perturbations corresponding to Chebyshev Figure 4.18 in terms of λ

Perturbation Δ_{pn}
0.044788
-0.012174
-0.054429
0.053791
-0.048585
0.041293
-0.042613
0.044244
-0.022856
0.034002
0.001992
-0.010983
-0.054355
0.050485
-0.054094
0.054906
-0.054765
0.052570
0.018351
-0.050925

Table 4.18: Perturbations corresponding to Chebyshev Figure 4.19 in terms of λ

Perturbation Δ_D
0.180619
0.172443
0.183713
-0.181037
-0.171314
0.183780
0.167170
-0.158295
0.181003
-0.180562
0.182222
0.163455
0.169033
-0.179975
-0.171585
-0.183148
-0.178462
0.184571
-0.172398
-0.181556

Table 4.19: Perturbations corresponding to Chebyshev Figure 4.20

Perturbation Δ_{pn}	Amplitude Perturbation Δ_A
0.186625	0.037950
0.181836	-0.056041
0.184329	-0.047026
0.189188	0.099475
-0.165948	-0.064183
0.181720	0.020054
0.137639	-0.069018
-0.157853	-0.032969
0.173126	0.033811
-0.144342	-0.098157
-0.168557	-0.042991
-0.147404	-0.042991
-0.185025	-0.081866
0.188597	0.009067
-0.164081	-0.082037
-0.173115	-0.098950
0.188806	0.092804
-0.186660	0.096045
0.189548	-0.038578
-0.189710	0.059075

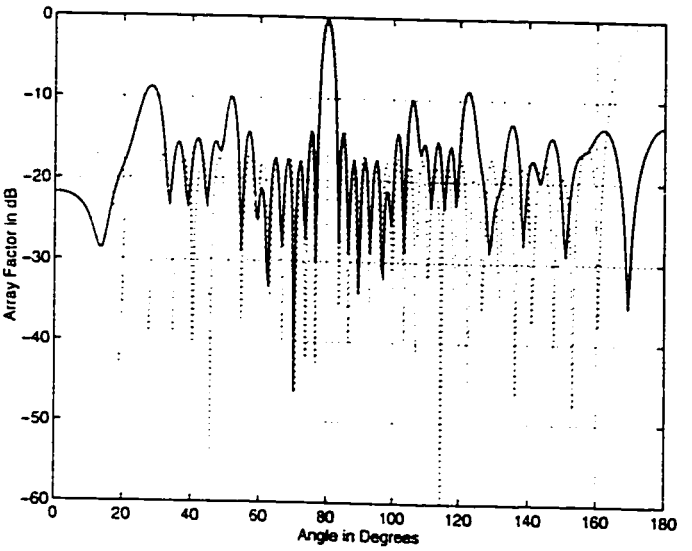

Figure 4.20: Array Factor Pattern for N=20, and separation=0.85λ with nulls imposed using complex weight perturbations at 165^0 and 175^0 with main beam at 80^0 and Control level chosen is $-15dB$.

4.5 Effect of grating lobe control on Directivity

An important reason for controlling grating lobes in scanned arrays is to increase the directivity of the array and thus, its overall gain. In this section we look at the behavior of directivity curves for various cases. At first, we look at the effect of grating lobe control on directivity, using complex weights and then that of position perturbations. For this, we consider a 12 element scanned array with main beam steered to 70^0. Figure 4.21 shows the variation of directivity as a function of inter-element spacing using complex weights. From this figure 4.21, we see that the curves (before and after null steering) are close to each other when the spacing is varied from 0.5λ to around 0.7λ. It is clear here that with increasing separation,

Table 4.20: Directivity for a 12 element array with main beam at 70^0 (using Complex Weights)

Spacing	D - Before	D - After
0.5λ	12.0	11.98
0.6λ	14.1	13.91
0.7λ	15.9	15.2
0.75λ	11.42	11.6
0.8λ	9.84	12.2
0.9λ	10.87	12.1

the directivity of the array also increases. At around 0.73λ, the directivity curve without grating lobe control, has a sudden drop, which shows that a grating lobe has appeared in the array factor pattern. Employing grating lobe control (from 0.75λ onwards), shows that the directivity curve is higher as compared to the curve obtained without grating lobe control. Thus, from these observations, we confirm that controlling of grating lobe provides for an increase in directivity. Figure 4.22 presents the variation of the directivity curves as a function of Element spacing when position perturbations are used for grating lobe control. Again, for a good comparison, we have used a 12 element array with main beam scanned to 70^0. The grating lobe appears at around 0.73λ, and it is from here that the curve that is generated after applying grating lobe control, moves a little higher as compared to the original, thereby showing an enhanced performance in this range.

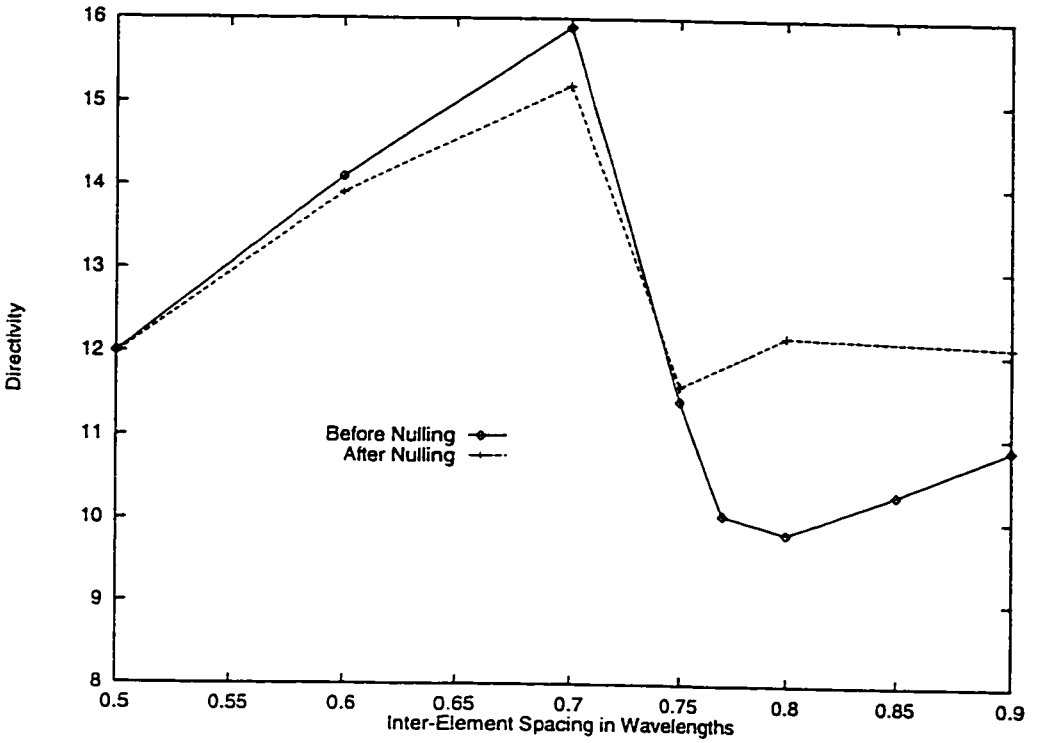

Figure 4.21: Directivity plot for a 12 element array whose main beam is at 70^0. Complex weights are used for null steering

Table 4.21: Directivity for a 12 element array with main beam at 70^0 (using Position perturbations)

Spacing	D - Before	D - After
0.5λ	12.0	12.07
0.6λ	14.1	13.8
0.7λ	15.9	15.19
0.75λ	11.42	12.1
0.8λ	9.84	12.5
0.9λ	10.87	12.8

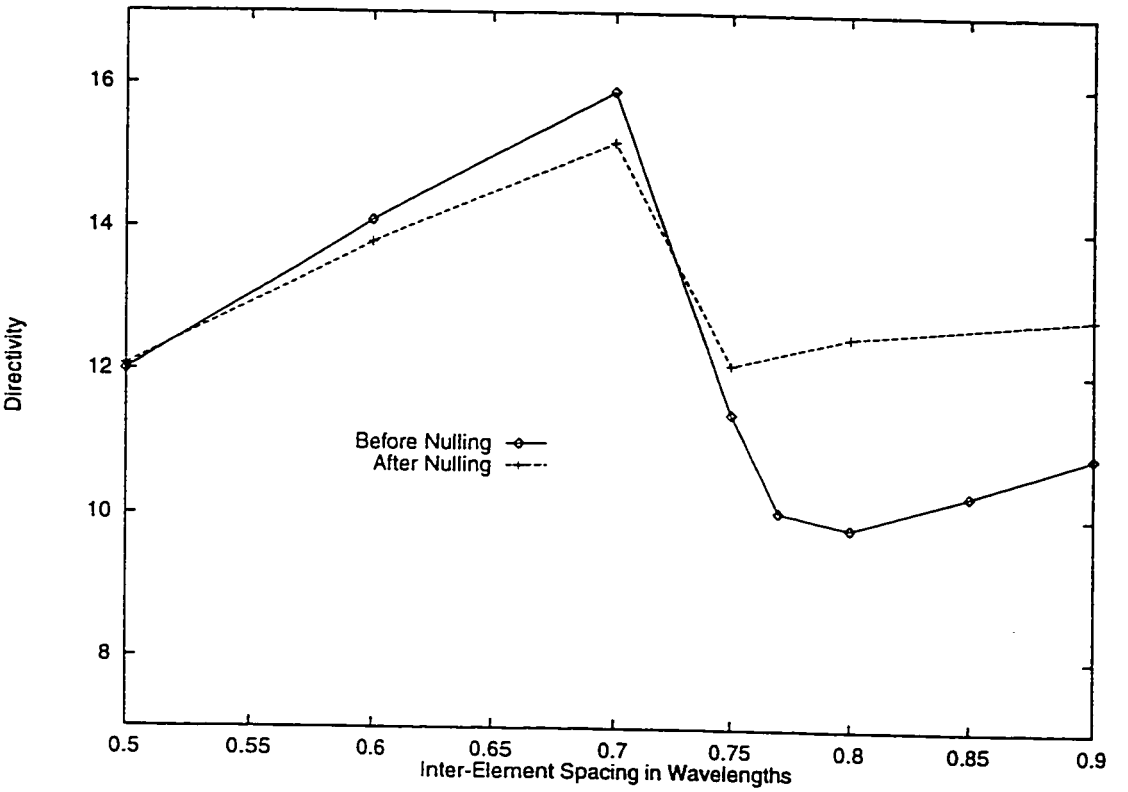

Figure 4.22: Directivity plot for a 12 element array whose main beam is at 70^0 and position perturbations are used for null steering

Table 4.22: Directivity for a 20 element Chebyshev array with main beam at 80^0 (using Position perturbations)

Spacing	D - Before	D - After
0.5λ	18.83	18.6
0.6λ	21.8	20.38
0.7λ	24.65	23.33
0.8λ	27.3	26.5
0.85λ	22.27	22.16
0.9λ	17.6	19.73

4.5.1 Directivity analysis for Chebyshev arrays

In this section the effect of application of the GA for controlling grating lobes in Chebyshev arrays is analysed with respect to changes in directivity. As seen from the figure 4.23 the curve before null steering and the curve after null steering are close to each other until 0.85λ, when grating lobe begins to appear. From 0.85λ onwards we see that controlling the height of the grating lobe by null steering results in an increase in the directivity of the array.

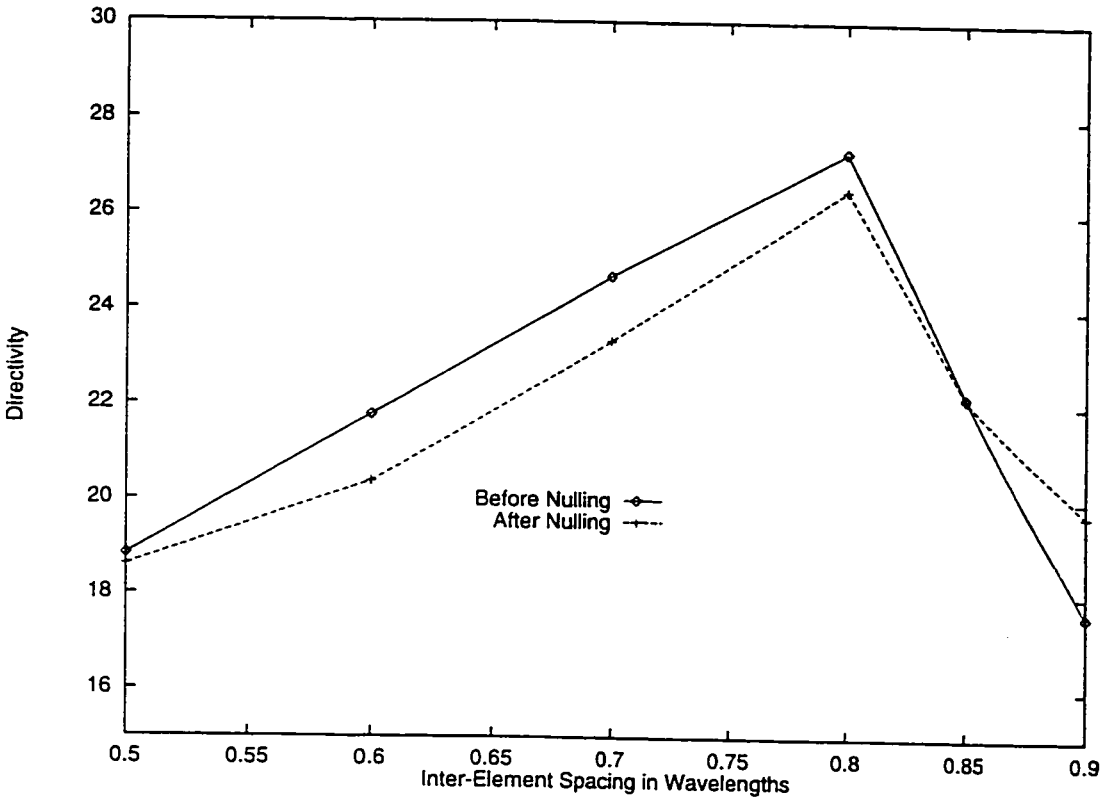

Figure 4.23: Directivity plot for a 20 element Chebyshev array whose main beam is at 80^0 and position perturbations are used for lobe control

Chapter 5

Effect of element pattern on grating lobe control

5.1 Introduction

The previous chapter has shown that controlling grating lobes using position perturbations is possible, but at the cost of getting patterns that have high side lobes. It is known from the literature that if the length of a finite length dipole is varied, the element pattern null position also shifts [33]. In this chapter we have used this element null synthesis technique, in order to control the grating lobe and get an overall resultant pattern whose side-lobe topology is close to the original. This would, be a very effective solution to the grating lobe problem.

5.2 Finite length dipole

In this section we analyse the radiation characteristics of a linear dipole of any length. To reduce the mathematical complexities, it will be assumed that the dipole has a negligible diameter.

5.2.1 Current distribution

For a very thin dipole, the current distribution at a point (x',y',z') can be written, to a good approximation, as

$$I_e(x', y', z') = \begin{array}{ll} \hat{a}_z I_0 sin[k(\frac{l}{2} - z')], & 0 \leq z' \leq l/2 \\ \hat{a}_z I_0 sin[k(\frac{l}{2} + z')], & -l/2 \leq z' \leq 0 \end{array} \tag{5.1}$$

This distribution assumes that the antenna is center-fed and the current vanishes at the end points ($z' = \pm l/2$). Experimentally it has been verified that the current in a center-fed wire antenna has sinusoidal form with nulls at the end points [33].

5.2.2 Radiated fields: Element factor, Space factor and Pattern multiplication

For the current distribution of equation 5.1, it is shown in [1] that closed form expressions for the E and H fields can be obtained which are valid for all regions (any observation point except on the source itself). The mathematical expression

for the electric field is given as:

$$E_\theta = \int_{-l/2}^{+l/2} dE\theta = j\eta \frac{ke^{-jkr}}{4\pi r} sin\theta [\int_{-l/2}^{+l/2} I_e(x', y', z') e^{jkz' cos\theta} dz'] \qquad (5.2)$$

The factor outside the brackets is designated as the *element factor* and that within the brackets as the *space factor*. For this antenna, the element factor is equal to the field of a unit length infinitesimal dipole located at a reference point (the origin). In general, the element factor depends on the type of current and its direction of flow while the space factor is a function of the current distribution along the source. The total field of the antenna is equal to the product of the element and space factors. This is referred to as *pattern multiplication* for continuously distributed sources, and it can be written as

$$Total field = [Element factor] \times [Space factor] \qquad (5.3)$$

The pattern multiplication for continuous sources is analogous to the pattern multiplication for discrete element antennas (arrays). For the current distribution of equation 5.1 equation 5.2 can be written as

$$E_\theta = j\eta \frac{kI_0 e^{-jkr}}{4\pi r} sin\theta [\int_{-l/2}^{0} sin[k(\frac{l}{2} + z')] e^{+jkz' cos\theta} dz' + \int_{0}^{l/2} sin[k(\frac{l}{2} - z')] e^{+jkz' cos\theta} dz'] \qquad (5.4)$$

Mathematically manipulating 5.4 we get the electric field as:

$$E_\theta = j\eta \frac{kI_0 e^{-jkr}}{2\pi r}\left[\frac{cos(\frac{kl}{2}cos\theta) - cos(\frac{kl}{2})}{sin\theta}\right] \tag{5.5}$$

Equation 5.5 is applicable to an element placed on the z-axis. The choice of a finite length dipole of length 1.0λ is suitable for the broadside case. When dealing with scanned arrays with large inter element spacing, we need to have element lengths greater than 1.0λ for grating lobe control. Practically, a co-linear array configuration is not feasible for such elements lengths. In order to use the element pattern in our work on scanned arrays, we include means to shift the maximum of the element pattern to a required direction. Physically, this amounts to placing the dipole at an angle α with respect to the z-axis. This modification can be added as the angle α that achieves this scanning, to equation 5.5 and is shown in equation 5.6

$$E_\theta = \left[\frac{cos(\frac{kl}{2}cos(\theta + \alpha)) - cos(\frac{kl}{2})}{sin(\theta + \alpha)}\right] \tag{5.6}$$

Figure 5.1 shows the geometry of an array of finite length dipoles placed at an angle of α with respect to z-axis. This array is practically realizable and also avoids the co-linear configuration.

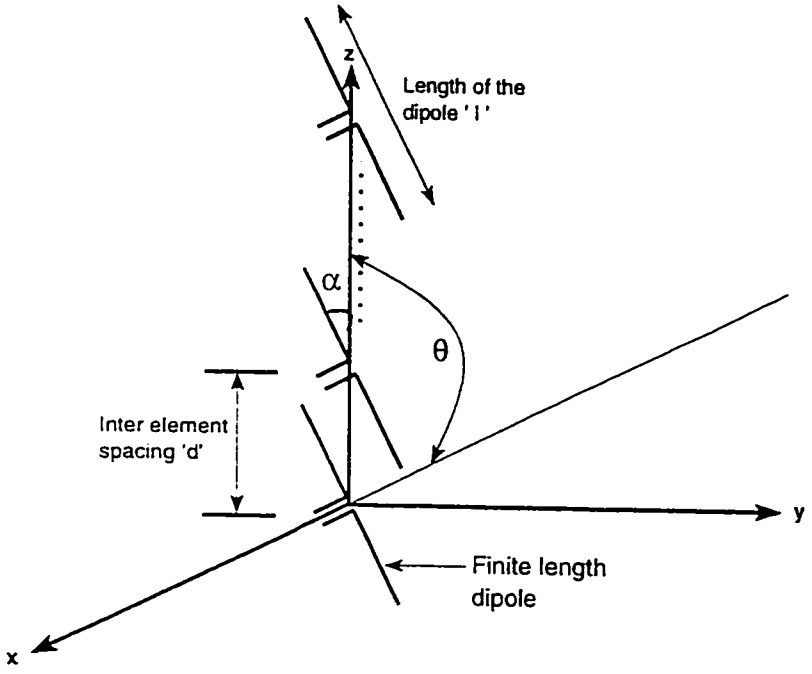

Figure 5.1: An array of dipoles placed at an angle α with respect to z-axis

5.3 Effect of increasing the length of dipole

In this section we discuss the effect of increasing the length of a dipole on the element pattern. Figure 5.2 shows the pattern of dipoles of lengths ranging from1.0λ, to 1.1λ , generated using equation 5.6 which are placed on the z-axis ($\alpha = 0$). For example, from figure 5.2(b) we see that choosing a length of 1.01λ produces an element pattern null at 168.5^0. It would be our endeavor to make use of such element nulls produced by choosing appropriate length of dipoles, in cancelling the grating lobe, using the pattern multiplication rule.

Let us now consider another example of the generated element pattern when the length of the dipole is changed to 1.07λ. Figure 5.3 (h) shows that an increase in the length of the dipole has caused the element null to shift to 150.5^0. This null is quite deep with a depth of more than $-60dB$.

In order to validate the achieved patterns we chose a dipole of length 1.25λ and generated an element pattern using equation 5.6. This is shown in figure 5.4. This element radiation pattern was compared with the reference element pattern available in Balanis [1]. The obtained plot was in agreement with the reference.

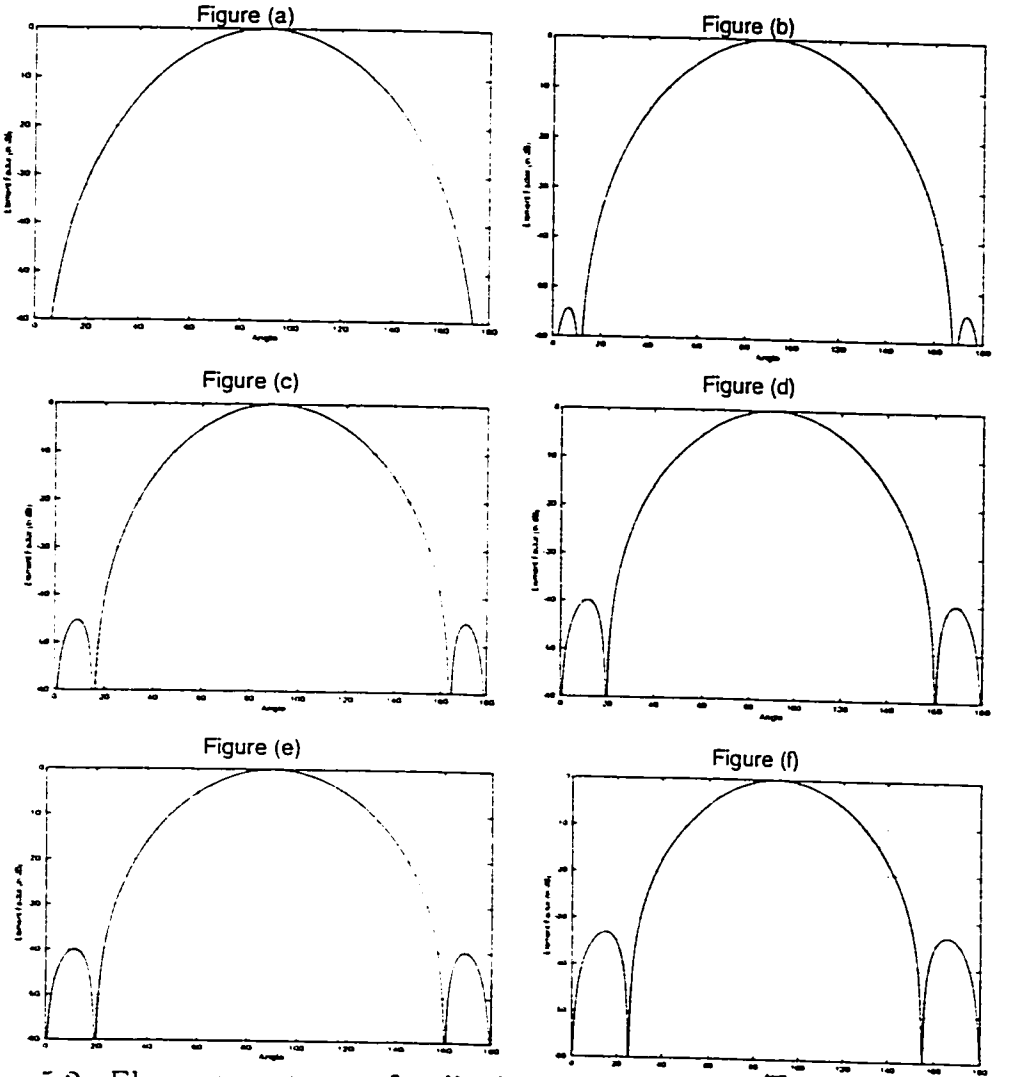

Figure 5.2: Element patterns of a dipole as its length is varied from1.0λ to 1.05λ. For Fig (a)L=1.0λ. For Fig (b) L=1.01λ. For Fig (c) L=1.02λ, For Fig (d) L=1.03λ. For Fig (e) L=1.04λ. and For Fig (f) L=1.05λ

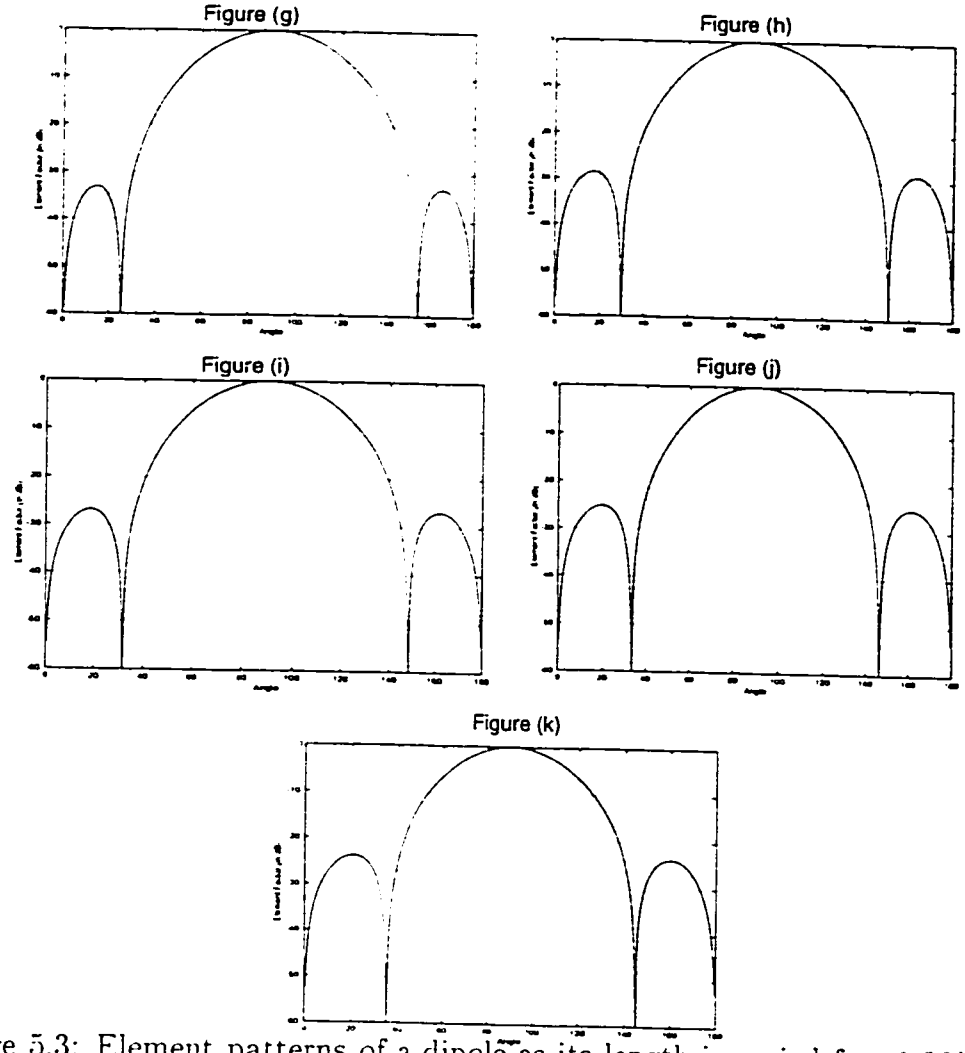

Figure 5.3: Element patterns of a dipole as its length is varied from1.06λ to 1.1λ. for Fig (g) L=1.06λ, for Fig (h) L=1.07λ, for Fig (i) L=1.08λ, for Fig (j) L=1.09λ, and for Fig (k) L=1.1λ

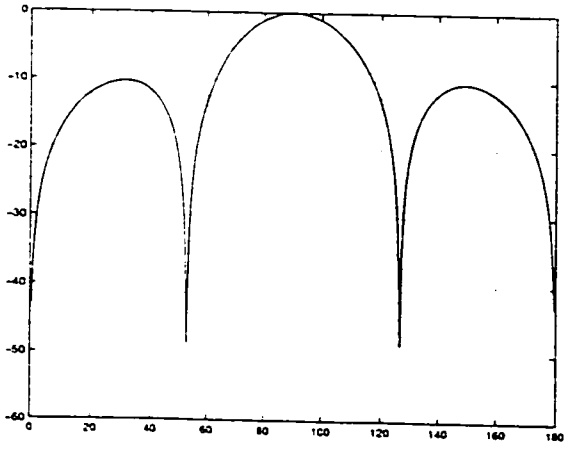

Figure 5.4: Element pattern of a dipole of length 1.25λ.

5.3.1 Scanning the element pattern

In this section we consider examples of scanning the element pattern. This has been done in order to study the effect of scanning the pattern on element nulls. Scanning is also important because we intend to apply these element patterns to control grating lobes in scanned arrays. Consider the first example of a dipole of length 1.04λ whose pattern has been scanned in steps from 0^0 up to 90^0. This scanning is achieved by choosing an appropriate value of α in equation 5.6. Another example shown is for a length of 1.05λ. Figures 5.5 and 5.6 show that as the pattern is scanned from 0^0 to 90^0, the position of the nulls also change. This is an important observation that can be used in choosing the desired length of the dipole in order to null the grating lobe. If we now increase the length of the dipole to 1.09λ with

$\alpha = 20^0$, we see that nulls of depth $-60dB$ at 13.5^0, 126.5^0 and 160^0. The height of the side-lobes is high as compared to the plot (b) of figure 5.6. These details are shown in figure 5.7. In order to have a good documentation, table 5.1 is provided showing the variation of null positions for dipoles of different lengths.

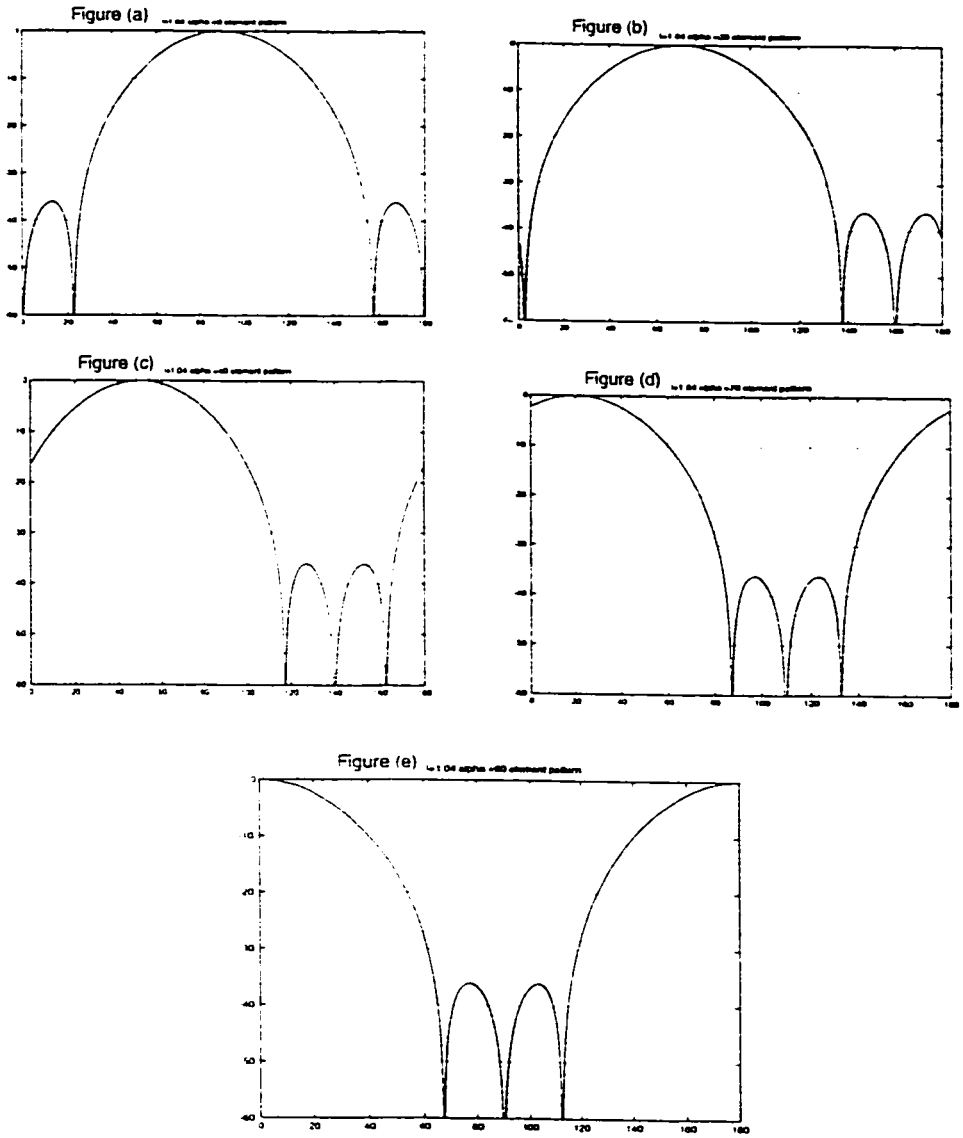

Figure 5.5: Element patterns of a dipole of length 1.04λ. Fig (a) is for $\alpha = 0^0$ Fig (b) is for$\alpha = 20^0$. Fig (c) is for $\alpha = 40^0$. Fig (d) is for $\alpha = 70^0$ and Fig (e) is for $\alpha = 90^0$.

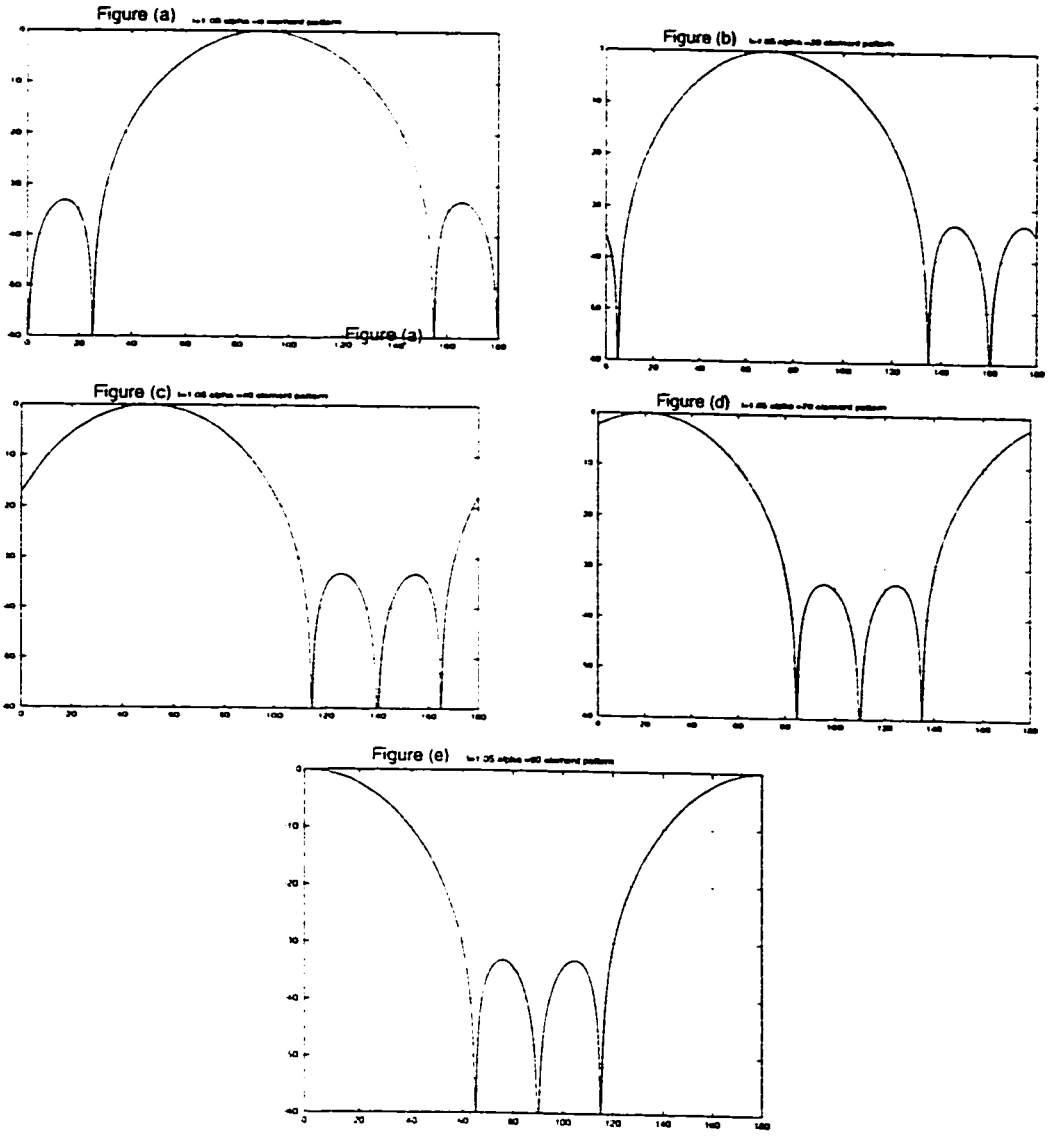

Figure 5.6: Element patterns of a dipole of length 1.05λ. Fig (a) is for $\alpha = 0^0$ Fig (b) is for$\alpha = 20^0$. Fig (c) is for $\alpha = 40^0$. Fig (d) is for $\alpha = 70^0$ and Fig (e) is for $\alpha = 90^0$.

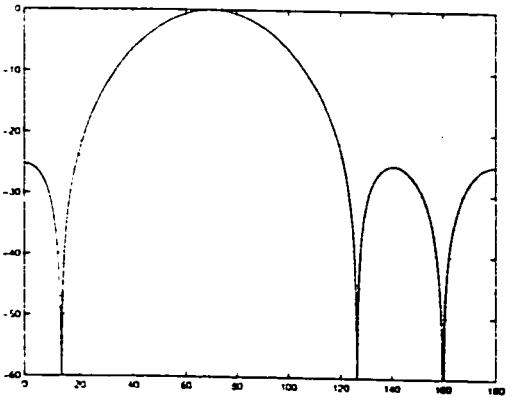

Figure 5.7: Element pattern of a dipole of length 1.09λ with $\alpha = 20^0$.

5.4 Application of Element pattern and Array factor pattern for grating lobe control

In this section we present the results obtained when we use both the element radiation pattern and array factor pattern to control grating lobes. Pattern multiplication rule would be applied to get the resultant radiation pattern.

5.4.1 Application to a 12 element 0.75λ spaced array

We first start with a 12 element array whose main beam is scanned to 70^0. The inter element spacing is 0.75λ. Figure 4.4 shows the use of position perturbations on the array factor pattern in order to control the grating lobe. As seen from figure 4.4, a grating lobe having a large width appears, with its maximum at 180^0. By choosing an appropriate element length, we could steer the element nulls, in addition to the array factor nulls generated by position perturbations, in order to effectively cancel it. An element length of 1.03λ is suitable in this case because it has element nulls at 140^0,160^0 and 180^0. Having these nulls, along with the array factor nulls at 150^0 and 160^0 clearly have resulted in the cancellation of the grating lobe. The shape of the resultant radiation pattern is also very much close to the original. Figure 5.8 shows the radiation pattern of the 12 element dipole array, each element of length 1.03λ in comparison with the unperturbed array factor pattern. The comparison shows that grating lobe present in the array factor pattern is effectively cancelled by multiplying

it with the element pattern of a dipole placed at an angle of 20^0 with respect to z-axis and of length 1.03λ. Figure 5.9 presents the radiation pattern of the same 12

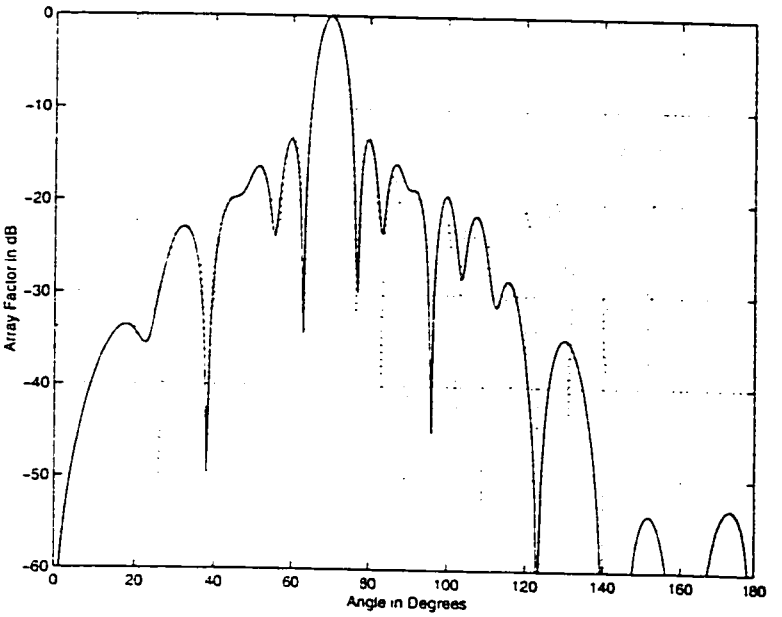

Figure 5.8: Radiation pattern of a 12 element array of dipoles, each of length 1.03λ and having array factor nulls at 160^0 and 170^0. Inter element spacing is 0.75λ. Dotted lines show the unperturbed array factor pattern

element array without position perturbations, having a spacing of 0.75λ and each dipole has a length of 1.03λ. This pattern is compared with the unperturbed array factor pattern. In this figure we see that the grating lobe is cancelled effectively due to the element nulls. The plot of figure 5.9 shows good improvement in the pattern shape as compared to the case where the grating lobe was controlled just by perturbing element positions of the array. Thus, this technique of choosing an element of a particular length to get nulls in the element pattern not only results in

Table 5.1: Table showing the variation of null positions for different dipole lengths when $\alpha = 20^0$.

Length of dipole	Null positions	Side-lobe level (in dB)
0.5λ	160^0	-
1.0λ	160^0	-
1.01λ	148.5^0,160^0,171.5^0	-54.371
1.02λ	144^0,160^0, 176^0	-45.283
1.03λ	140^0,160^0,180^0	-39.930
1.04λ	137.5^0,160^0,2.5^0	-36.111
1.05λ	135^0,160^0,5^0	-33.143
1.07λ	130.5^0,160^0,9.5^0	-28.620
1.09λ	126.5^0,160^0,13.5^0	-25.200
1.10λ	125^0,160^0,15^0	-23.742
1.15λ	117.5^0,160^0,22.5^0	-18.000
1.20λ	112^0,160^0,28^0	-13.800
1.25λ	107^0,160^0,33^0	-10.325

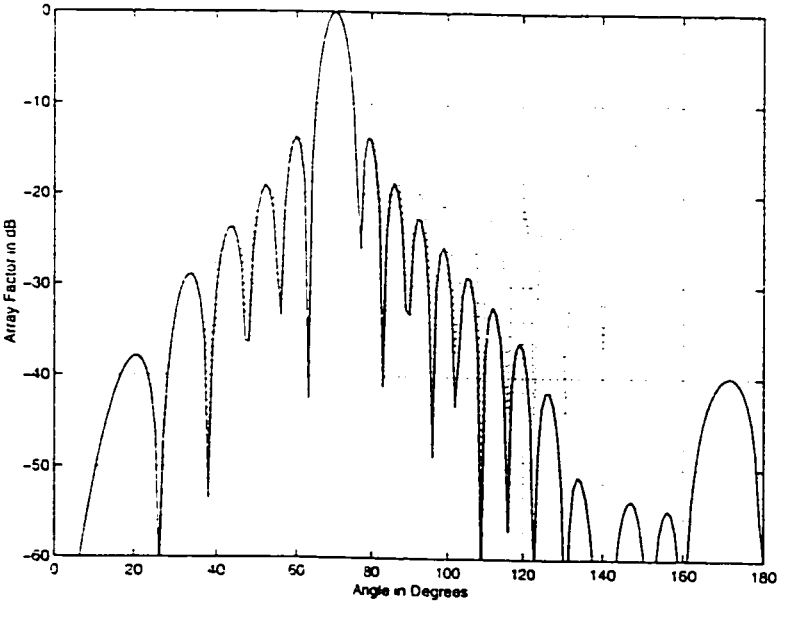

Figure 5.9: Radiation pattern of a 12 element array of dipoles, each of length 1.03λ. Inter element spacing is 0.75λ. Dotted lines show the array factor pattern.

cancellation of grating lobes. but also gives satisfactory radiation patterns.

5.4.2 Application to 12 element, 0.8λ spaced array

In this section we extend the use of the element pattern to a 12 element array whose main beam is scanned to 70^0 and which has an inter-element spacing of 0.8λ. From figure 4.5 we see that the grating lobe shifts its position when the spacing is increased from 0.75λ to 0.8λ. Because of this shift in the position of the grating lobe. we need to choose the dipole element's length that produces element nulls in the direction of the grating lobe. The optimum length of the dipole that produces element nulls in the direction of the grating lobe is 1.05λ. This dipole is at an angle of $\alpha = 20^0$ with the z-axis. The angles at which nulls are produced are 135^0. 160^0 and 5^0. Grating lobe control using element position perturbations is employed at 150^0 and 160^0. The combined effect of these is shown in figure 5.10. Figure 5.11 compares the overall radiation pattern with the unperturbed array factor pattern. Here. grating lobe control is done using the element pattern nulls alone. Each plot shows that the new radiation pattern has very good side lobe structure and effective cancellation of the grating lobe.

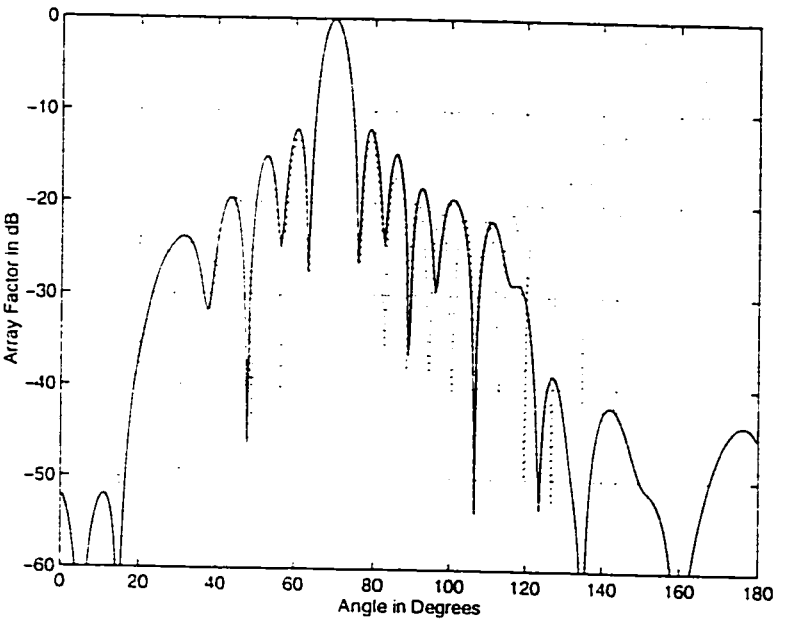

Figure 5.10: Radiation pattern of a 12 element array of dipoles, each of length 1.05λ and having array factor nulls at 150^0 and 160^0. Inter element spacing is 0.8λ. Dotted lines show the unperturbed array factor pattern

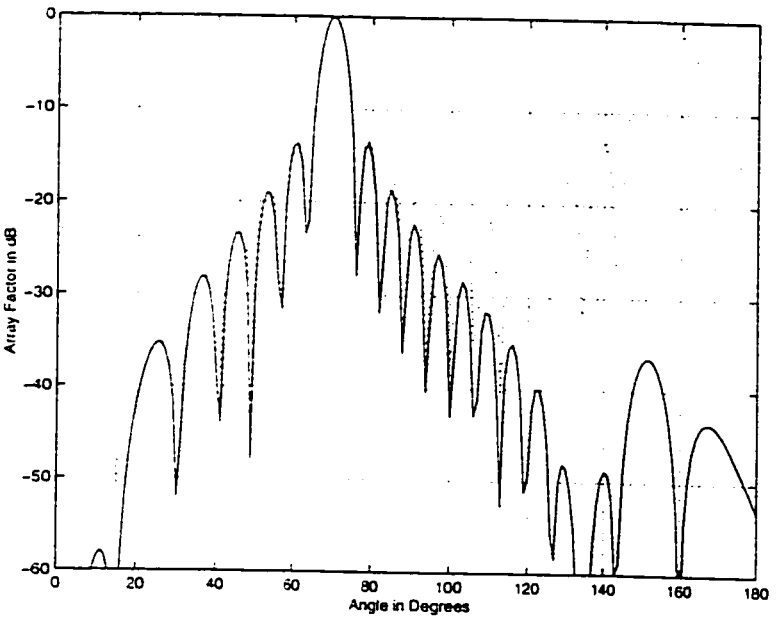

Figure 5.11: Radiation pattern of a 12 element array of dipoles, each of length 1.05λ. Inter element spacing is 0.8λ. Dotted lines show the array factor pattern.

5.4.3 Application to a 20 element array

In this section we show the application of the pattern multiplication rule for a 20 element array whose main beam is scanned to 60^0. The inter-element spacing is 0.75λ. Grating lobe appears in the array factor pattern with its maximum at 146^0. We have chosen an element of length 1.04λ and oriented at $\alpha = 30^0$ with the z-axis. This configuration of the element produces nulls in directions 127.5^0, 150^0 and 172.5^0 and hence is effective in cancelling the grating lobe. Figure 5.12 shows the radiation pattern of this array in comparison to the unperturbed AF pattern. Figure 5.13 shows the radiation pattern produced with the usage of element pattern nulls only in comparison with the array factor pattern. These figures show that the resultant

radiation pattern again has a very good side-lobe topology and effective grating lobe cancellation

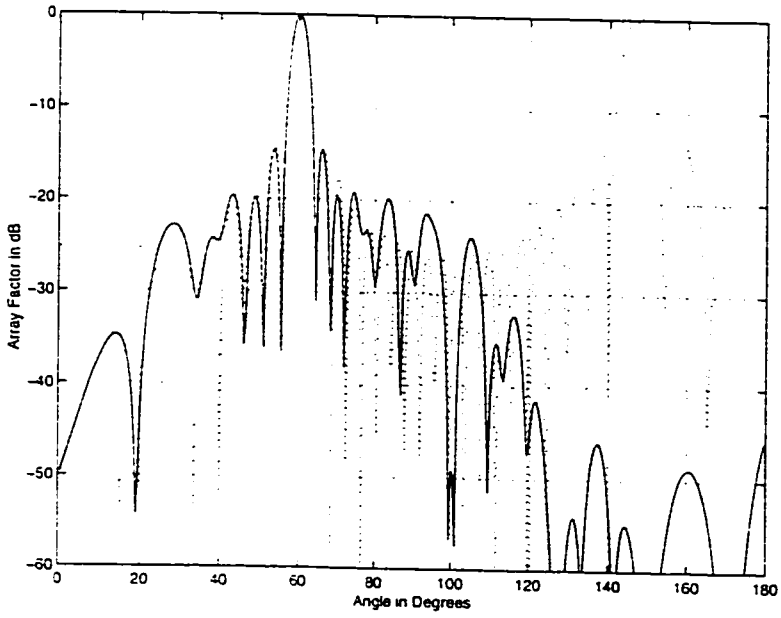

Figure 5.12: Radiation pattern of a 20 element array of dipoles, each of length 1.04λ and having array factor nulls at 144^0 and 148^0. Inter element spacing is 0.75λ. Dotted lines show the original array factor pattern.

5.4.4 Application to a Chebyshev array

As a final example, the pattern synthesis method is applied to a 20 element Chebyshev array with a side-lobe level of -18dB. The main beam of this array is scanned to 80^0 and the inter-element spacing is 0.85λ. The grating lobe just appears in the pattern, and therefore element nulls are needed to eliminate it. A dipole length of 1.005λ placed at $\alpha = 10^0$ is found suitable for this case. Figures 5.14 shows that

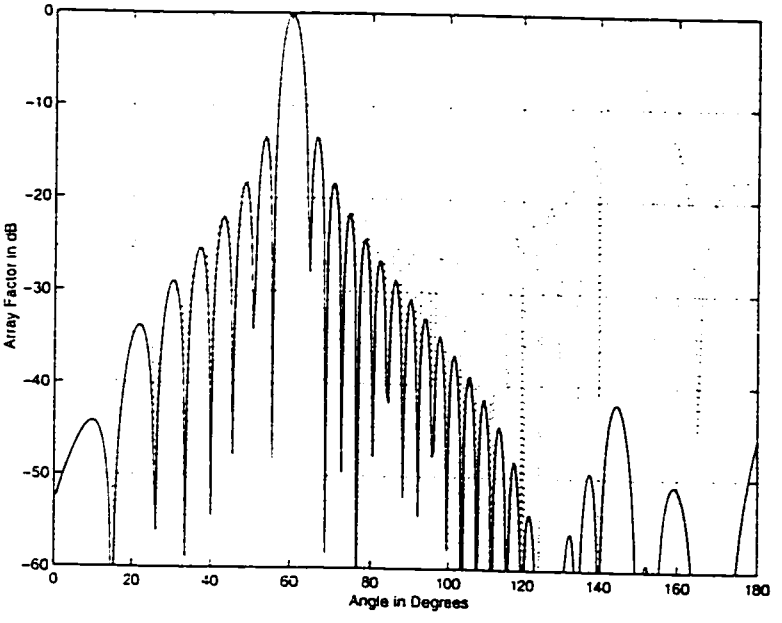

Figure 5.13: Radiation pattern of a 20 element array of dipoles, each of length 1.04λ. Inter element spacing is 0.75λ. Dotted lines show the array factor pattern.

the resultant radiation pattern has no grating lobe, but the side lobe structure is changed from the original, where all side lobes have the same level.

5.5 Discussion

Our main purpose of providing an effective solution to the grating lobe problem led to the utilization of element factor nulls. Their use, not only eliminates the grating lobes but also gives good resultant radiation patterns. The flexibility of synthesizing the element factor nulls by choosing appropriate lengths of the dipole elements makes practical application of the technique, feasible. As shown, this

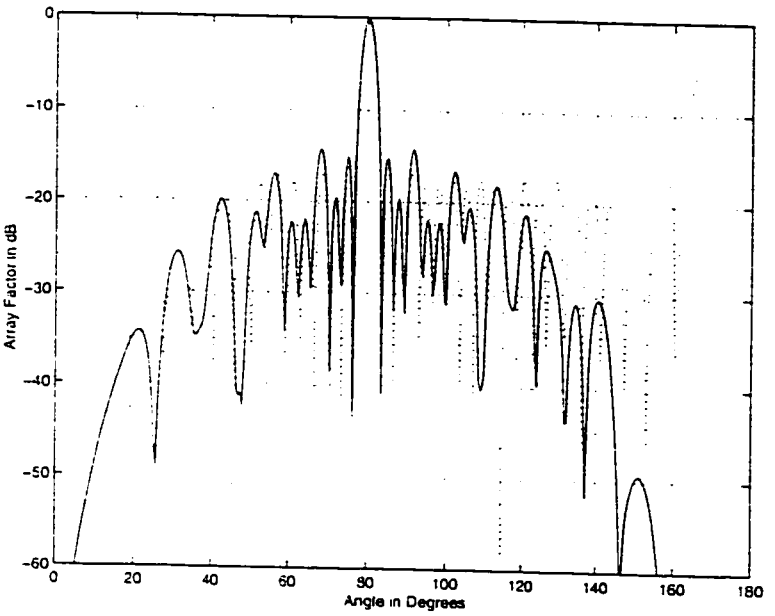

Figure 5.14: Radiation pattern of a 20 element Chebyshev array of dipoles, each of length 1.005λ and having array factor nulls at 165^0 and 175^0. Inter element spacing is 0.85λ. Dotted lines show the original array factor pattern.

method can be applied to any linear array. Side-lobe structure of the resultant radiation pattern is also good. Effective control of the grating lobe is thus made possible with this technique. Hence, this method provides a very good solution to the grating lobe problem.

Chapter 6

Conclusions and Recommendations

6.1 Conclusion

In this work, application of the genetic algorithm for null steering to control grating lobes has been studied and developed. Element position perturbations and complex weight variations are null steering techniques that have been employed to achieve grating lobe control. These techniques provide grating lobe control at the specified directions and achieve the required depths, but the resultant pattern is a little disturbed as compared to the original. In order to get a radiation pattern that has a good side-lobe topology and a controlled grating lobe level, use of a finite length dipole element pattern has been investigated. This synthesis technique is based on

the usage of element pattern nulls. These element nulls are a function of the length of the dipole and by choosing an appropriate element, these nulls can be placed in the vicinity of the grating lobe in order to control it. Results have been presented for both uniform and non-uniform arrays, using the GA based control as well as control based on element pattern synthesis. The following are the conclusions drawn from the study.

- The number of iterations and hence computation time needed to control grating lobes is large as compared to null steering in the directions of sidelobes. For example, the number of generations needed for steering two nulls using position perturbations in the pattern of a broadside array having an inter-element separation of 0.5λ is 153 as compared to 2589 generations needed to control grating lobe in a scanned array (main beam at 70^0) with 0.75λ separation. For the same cases when complex weights are used, the number of generations needed are 294 and 9688 respectively, thus showing that use of complex weights slows the rate of convergence.

- Mathematical approximations that are required for getting an analytical solution, are not needed for null steering using either complex weights or position perturbations when using the genetic algorithm.

- Complex weights have not provided any other specific advantages over position perturbations vis-a-vis directivity, or improvement in pattern structure, when

used for grating lobe control. Practically, position perturbations can be used because fewer variables need to be controlled.

- The appearance of the grating lobes into the visible region causes a sharp drop in directivity. This study has shown that by reducing grating lobe levels, the directivity of the array increases.

- Application of grating lobe reduction to Chebyshev arrays also led to patterns with increased directivity.

- Grating lobe control using the genetic algorithm can easily be applied to any array type simply by changing the fitness function.

- Null steering to control grating lobes does not affect the main beam.

- Use of null steering for grating lobe control in arrays with large inter-element separation results in patterns with high side lobes. Further control of grating lobes can be achieved using a suitable element factor.

- The element pattern synthesis method used is based on choosing an appropriate length of dipoles for getting element nulls in the direction of the grating lobe. This technique is simple in design and practical to implement.

- Array factor grating lobe control using null steering together with the appropriate element factor results in a useful array pattern where the array factor

control reduces the grating lobe level while the element factor helps to constrain the grating lobe and side lobes in other directions.

- The use of the element pattern nulls provides a good solution to the grating lobe problem. The obtained results show that the resultant radiation pattern has good side-lobe structure and a controlled level of the grating lobe.

Thus, the genetic algorithm has been used to provide precise solutions for null steering by element position control and complex weight variations. Processing times are also quite small.

The advantages derived by controlling the level of the grating lobes are manifold.

- Firstly the scan angle range increases. This is of vital importance in areas such as Radar and phased array systems.

- When large phased arrays with reduced grating lobes are used, we get multiple advantages such as increased directivity and greater scan range thereby making the system cost effective.

Although the results in this work are based on the linear arrays, both uniform and non-uniform, this technique is general, and may be applied to arbitrary geometries. Hence, the use of the genetic algorithm is an advantageous proposition for designers, in particular, for those who wish to evolve suitable and cost effective solutions for antenna array problems. When combined with the element pattern synthesis technique, it provides an effective solution to pattern shaping problems.

6.2 Recommendations

After conducting a detailed investigation of controlling grating lobes we provide the following recommendations and direction for future research.

- A practical implementation of a scanned array can be attempted which has a pattern with controlled grating lobes, based on the results of this work.
- The genetic algorithm can be implemented using other forms fitness functions that not only control grating lobes, but also constrain the side-lobe levels within a desired range.
- Application of the genetic algorithm to control grating lobes in 2D arrays is also an advantageous proposition.
- Investigation of element patterns of different element types could be undertaken for grating lobe control.

Bibliography

[1] Balanis, Constantine, A. . *Antenna Theory Analysis and Design* . John Wiley and Sons, New York., 2nd edition, 1982.

[2] T.H Ismail. *Null steering in phased and adaptive arrays by controlling the element positions.* PhD thesis, KFUPM, Dhahran, Saudi Arabia, Aug 1991.

[3] Dawoud, M. M.: Tennant, A.: Anderson, A. P. Null steering and pattern synthesis of array antennas by genetic algorithms. *IEE Conference Proceedings. Microwaves 94*, pages 112-116, 1994.

[4] Goldberg, D.E. . *Genetic algorithms in search, optimization, and machine learning* . Addison Wesley, 1989.

[5] Schelkunoff, S. A. A mathematical theory of linear arrays. *Bell System Technical Journal*, 22:80–107, 1943.

[6] Vu, T. B. Method of null steering without using phase shifters. *IEE Proceedings Part H*, 131:242-246, Aug 1984.

[7] Ismail, T.H: Dawoud, M.M. Null steering in phased arrays by controlling the element positions. *IEEE Transactions on Antennas and Propagation*, AP-39(11):1561-1566, Nov 1991.

[8] Dawoud, M. M.: Ismail, T. H. Experimental verification of null steering by element position perturbations. *IEEE Transactions on Antennas and Propagation*, 40(11):1431-1434, Nov 1992.

[9] Vu, T. B. Null steering in phased arrays: A brief review of the basic principles and potential applications. *Asia-Pacific Journal (Part A)*, 1(2):151-171, 1991.

[10] Dawoud, M. M. Null steering in scanned linear arrays by element position perturbations. *International Journal of Electronics*, 78(4):743-757, 1995.

[11] Hu, Jin-Lin.: Ma, Yan: Lin, Shi-Ming. Deep null steering by controlling excitation phases of part elements. *International Journal of Electronics*, 83(5):660-664, 1997.

[12] Ko, C. C. A fast null steering algorithm for linearly constrained adaptive arrays. *IEEE Transactions on Antennas and Propagation*, 39(8):1098-1104, Aug 1991.

[13] Nagesh, S. R.; Vedavathy, T. S. Procedure for synthesizing a specified sidelobe topography using an arbitrary array. *IEEE Transactions on Antennas and Propagation*, 43(7):742-745, Jul 1995.

[14] Mismar, M. J.; Ismail, T. H. Null steering using the minimax approximation by controlling only the current amplitudes. *International Journal of Electronics*, 78(2):409–415, Feb 1995.

[15] Wu, Lixue; Zielinski, Adam; Bird, John S. Synthesis of shaped radiation patterns using an iterative method. *Radio Science*, 30(5):1385–1392, Sep - Oct 1995.

[16] Dawoud, M. M.; Tennant, A.; Anderson, A. P. Null steering in adaptive arrays using a genetic algorithm. *Proc. 24th European Microwave Conference*, 2:1108–1114, Sep 5-8 1994.

[17] Johnson, J.M ; Rahmat-Samii, Y. Genetic Algorithms in Engineering Electromagnetics. *IEEE Antennas and Propagation Magazine*, 39(4):7–21, 1997.

[18] Marcano, D.; Jimenez, M.; Chang, O.; Duran, F. Application of genetic algorithms for the synthesis of linear antenna arrays. *Proc 1996 3 Int Congr Numer Methods Eng Appl Sci CIMENICS 96*, pages 257–263, 1996.

[19] Haupt, Randy L. Thinned arrays using genetic algorithms. *IEEE Transactions on Antennas and Propagation*, 42(7):993–999, Jul 1994.

[20] Lu, Yilong; Yan, Keen Keong. Genetic algorithms based pattern synthesis approach for arbitrary array design. *Annual Review of Progress in Applied Computational Electromagnetics*, 2:734–741, 1996.

[21] Tennant, A.; Dawoud, M. M.; Anderson, A. P. Array pattern nulling by element position perturbations using a genetic alogrithm. *Electronics Letters*, 30(3):174–176, Feb 3 1994.

[22] Haupt, Randy L. Speeding convergence of genetic algorithms for optimizing antenna arrays. *Annual Review of Progress in Applied Computational Electromagnetics*, 2:742–749, 1996.

[23] Johnson, J. Micheal; Rahmat-Samii, Yahya. Genetic algorithm optimization for aerospace electromagnetic design and analysis. *IEEE Aerospace Applications Conference Proceedings*, 1:87–102, 1996.

[24] Ares, F.; Rengarajan, S. R.; Villanueva, E.; Skochinski, E.; Moreno, E. Application of genetic algorithms and simulated annealing technique in optimising the aperture distributions of antenna array patterns. *Electronics Letters*, 32(3):148–149, Feb 1 1996.

[25] Chambers, B.; Anderson, A. P.; Mitchell, R. J. Application of genetic algorithms to the optimization of adaptive antenna arrays and radar absorbers. *IEE Conference Publication*, 1(414):94–99, 1995.

[26] Marcano, D.; Duran, F.; Chang, O. Synthesis of multiple beam linear antenna arrays using genetic algorithms. *IEEE Antennas and Propagation Society, AP-S International Symposium(Digest)*, 2:938–941, 1995.

[27] Proukakis, Christos: Manikas, Anthanassios. Study of ambiguities of linear arrays. *Proceedings - ICASSP, IEEE International Conference on Acoustics, Speech and Signal Processing*. 4:549–552, 1994.

[28] Ragheb, H. A.: Shafai, L. Array thinning in phased arrays using dual mode horns. *AP-S International Symposium (Digest) - Antennas and Propagtion - 1989*, 3:1447 - 1450, 1989.

[29] Shafai, L. Scan gain enhancement in phased arrays by element pattern synthesis. *IEE Conference Publication*, 2(333):914–917, 1991.

[30] Rew, C. Y.: Park, S. B.: Ra, J. B. Elimination of all grating lobes in ultrasonic synthetic focusing using a linear array. *Electronics Letters*, 29(19):1729–1731, Sep 17 1993.

[31] Sharma, S. B.; Calla, O. P. N. Occurance of grating lobes and their suppression in broad wall slotted array of shunt slots. *Journal of the Institution of Electronics and Telecommunication Engineers*, 35(3):153–159, May-Jun 1989.

[32] Lockwood, Geoffery R.: Li, Pai-Chi; O'Donnell, Matthew; Foster, F. Stuart. Optimizing the radiation pattern of sparse periodic linear arrays. *IEEE Transactions on Ultrasonics, Ferroelectrics, and Frequency Control*, 43(1):7–14, Jan 1996.

[33] Murino, Vittorio: Trucco, Andrea: Regazzoni, Carlo S. Synthesis of unequally spaced arrays by simulated annealing. *IEEE Transactions on Signal Processing*, 44(1):119–123, Jan 1996.

[34] Stuckman B.E. ; Hill J.C. Method of null steering in phased array antenna systems. *Electronics Letters*, 26(15):1216–1218, 1990.

[35] Steinberg, B.D . *Principles of aperture and array system design*. John Wiley and Sons, New York, 1976.

[36] Stutzman, Warren L; Thiele, Gary A . *Antenna Theory and Design* . John Wiley and Sons, New York., 1981.

[37] Steyskal, H. Synthesis of antenna patterns with prescribed nulls. *IEEE Transactions on Antennas and Propagation*, AP-30:273–279, Mar 1982.

[38] Ares, F; Moreno, E. New method for computing Dolph-Chebyshev arrays and its comparison with other methods. *IEE Proceedings, Part H: Microwaves, Antennas and Propagation*, 135(2):129–131, 1988.

Vita

- Syed Tariq Magrabi
- Born in Hyderabad, India on the 13^{th} of November
- Received Bachelor's degree in Electronics and Communication Engineering from Osmania University Hyderabad, India in July, 1994.
- Worked as a Research and Development Engineer in M/s Aishwarya Telecom (P) Ltd.,Hyderabad from Aug. 1994 - Aug, 1995.
- Completed Master's degree in Electrical Engineering from King Fahd University of Petroleum and Minerals, Dhahran, Saudi Arabia in May, 1998.

IMAGE EVALUATION TEST TARGET (QA-3)

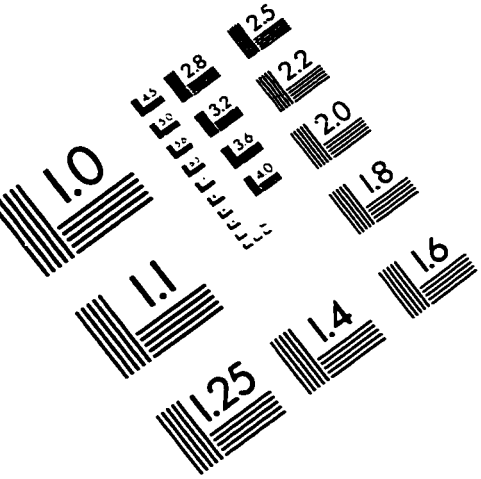

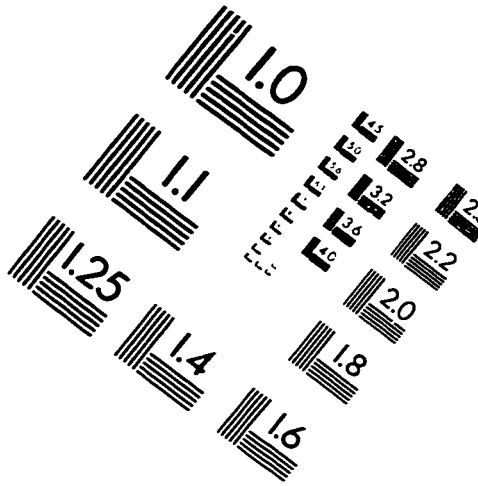

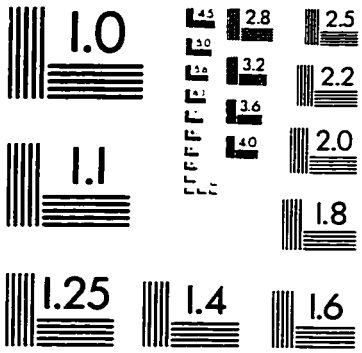

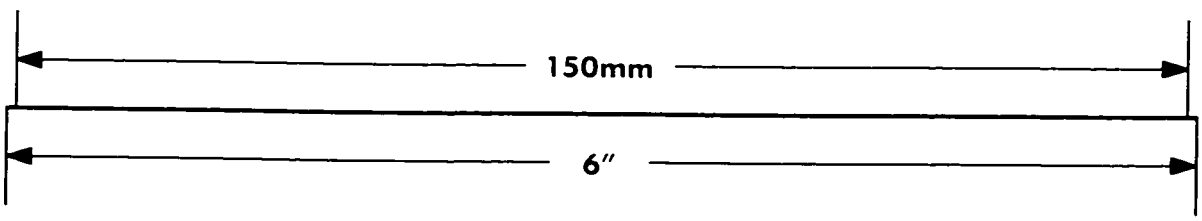

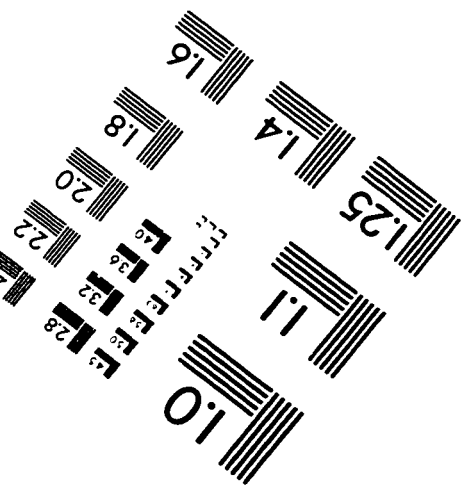

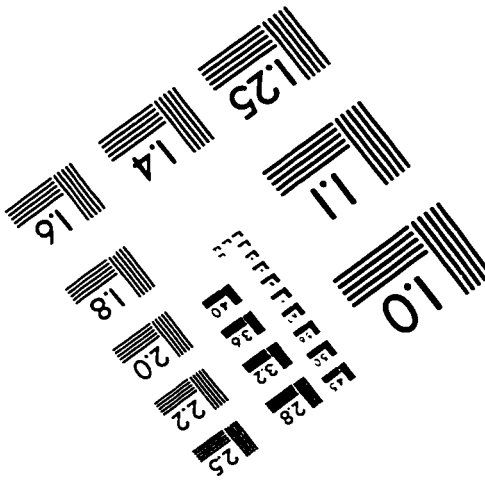

APPLIED IMAGE, Inc
1653 East Main Street
Rochester, NY 14609 USA
Phone: 716/482-0300
Fax: 716/288-5989